Hindawi
International Journal of Antennas and Propagation
Volume 2019, Article ID 7918765, 25 pages
https://doi.org/10.1155/2019/7918765

Review Article

Ultra-Wideband Antennas for Wireless Communication Applications

Tale Saeidi,[1] **Idris Ismail**,[1] **Wong Peng Wen**,[1] **Adam R. H. Alhawari**,[2] **and Ahmad Mohammadi**[3]

[1]*Electrical and Electronic Engineering Department of Universiti Teknologi PETRONAS, 32610 Bandar Seri Iskandar, Perak, Malaysia*
[2]*Electrical Engineering Department, College of Engineering, Najran University, Saudi Arabia*
[3]*Department of Electrical and Computer Engineering, Buein Zahra Technical University, Buein Zahra, Qazvin, Iran*

Correspondence should be addressed to Tale Saeidi; gs32772@gmail.com

Received 29 June 2018; Revised 2 October 2018; Accepted 18 October 2018; Published 22 April 2019

Academic Editor: N. Nasimuddin

A review paper concerning wide-band and ultra-wideband (UWB) antennas used for wireless communication purposes in terms of the materials as well as a numerical analysis is presented. These antennas which are taken into account are listed as wide-band microstrip antenna, wide-band monopole antenna over a plate, wide-slot UWB antenna, stacked patch UWB antenna, taper slot (TSA) UWB antenna, metamaterial (MTM) structure UWB antennas, elliptical printed monopole UWB antenna, and flexible wearable UWB antenna. The antennas' performance is compared based on their size and how they can be applicable for portable communication device applications. This review paper furnishes a proper direction to select varieties of figures in terms of impedance bandwidth, gain, directivity, dimensions, time domain characteristics, and materials affecting these antenna's characteristics.

1. Introduction

Antennas are known as a device which can send and receive signals. Hence, the speed of this send and receive process is a challenging interest especially when fast development of communication technologies matters. On the other hand, the swift development of the communication systems, both fixed and portable, required high data rate transition for a more covering area due to the network user increment. Thus, they needed a broad bandwidth (BW) to cover mobile and all wireless services. This can be possible by using wide-band and ultra-wideband (UWB) antennas with low profile to reduce the complexity and the fabrication cost [1].

This article provides the state of the art on the field of UWB antennas designed for wireless communication applications. It systematically reviews progress of the field within 10 previous years until the latest reported in a thorough overview for the advantage of the field readership, especially critically highlighting the untouched existing gaps that showed the necessity for new endeavour in exploring novel answers for these possible research questions. It concludes research insight for future research directive suggestions such as how loading can affect and improve the BW for wide-band and UWB antennas and how it can keep the antenna dimensions miniaturized while the antenna characteristics are not affecting a lot.

Before start designing the wide-band and UWB antennas, the design principles, procedures, and antennas' characteristics should be considered and known. Moreover, the microstrip antennas' design techniques, different structures and shapes, analysis, and feeding methods apply to improve the antennas' characteristics and performances. The microstrip patch antenna is the best selection for the researcher because of many advantages such as being a low-cost material, being lightweight, and also being easy to fabricate. Many researchers had improved the parameter result to give a

better performance and efficiency of the patch antenna design. The parameters that can be considered to improve are return loss, gain, directivity, and bandwidth [2, 3].

To design and apply the UWB antenna, the related working BW should be considered according to the Federal Communications Commission (FCC) and the required frequency bandwidth area. For example, the UWB standard used in USA and Canada is 3.1-10.6 GHz (Table 1) which is unlicensed and has no restrictions on the BW [4]. In [5], many UWB antennas were presented and then their design procedure, techniques, contributions, and performances were investigated.

The antenna used for communication applications was preferred to be of one of the following types: 3D, 2D, and planar. Choosing these antennas depends on their applications' requirements [6]; for instance, some of them are going to be taken for stabile devices and the others for portable devices. In some other applications like antennas used for mobile devices and wireless sensors on body networks, the trancievers should be in low profile to consume less area of printing board. Furthermore, for wireless body networks, antennas should be more flexible when they have to bend even close to 90 degrees [7, 8].

Overall, the transceiver systems applied for communications are listed as follows: wide-band microstrip, wide-band monopole antenna over a plate, wide-slot UWB antenna, stacked patch UWB antenna, taper slot (TSA) UWB antenna, elliptical printed monopole UWB antenna, metamaterial (MTM) structure UWB antennas, and dielectric resonator antennas (DRAs). These antennas have been changed based on the need to improve their performances accordingly.

The dielectric resonator (DR) can be used as an antenna which is called DRA. DRs are dielectric materials which are able to resonate at a certain frequency. These structures showed a high Q-factor and works at certain frequencies. In order to have radiation from DRA, it should contain a DR, a ground (GND) plane, and an excitation source [9]. More details and references in different shapes and performances are presented in Section 10.

A comprehensive review of recent scientific articles of the last 10 years was presented in this paper to provide antenna designers a valuable tool in their designing process and showing techniques in widening BW. This paper was emphasised mostly on antenna geometries, radiation characteristics, widening BW techniques, materials, and numerical tools applied to design the antennas.

The UWB standards in different countries are shown in Table 1 for a better understanding of UWB working BW in various countries.

This article is organized in 10 sections. Following an introduction about communication technology and antenna importance, some wide-band and UWB antennas are presented in Section 2 for communication technology. Section 3 illustrates the characteristics of monopole antenna when they were over a metallic plate. Thereafter, Sections 4, 5, and 6 demonstrate the wide-slot monopole antennas, the stacked patch antennas, and tapered slot monopole antennas' (TSA) specifications. Then, metamaterial (MTM) structure UWB antennas, printed elliptical monopole UWB antennas, wearable flexible UWB antennas, and DRA UWB antennas are presented in Sections 7, 8, 9, and 10, respectively. Finally, Section 11 concluded and explained which type of UWB antennas had better performances in terms of the aforementioned characteristics.

Table 1: UWB standards [1].

Country	Frequency bands
America, Canada	3.1-10.6 GHz No restrictions
Europe	3.1-4.8 GHz, avoid restrictions 6-8.5 GHz with no restrictions
Japan	3.4-4.8 GHz with detect-and-avoid (DAA) restriction 7.2-10.2 GHz with no restrictions
Korea	3.1-4.8 GHz with DAA restrictions 7.2-10.2 GHz no restrictions
Singapore	6-9 GHz no limitations 3.4-4.2 GHz with DAA limitations

2. Wide-Band Microstrip Antennas

The microstrip radiators were initially introduced in 1953 [4]. Then their properties and features were investigated for some years, and that was a spark to the microstrip concept's development [10]. Microstrip antennas had three definite parts as patch resonator, substrate, and ground (GND) plane. Due to the microstrip antennas' advantages such as being light, having a low profile, being low-cost, and having ease of fabrication, the interest on applying these antennas for industrial and scientific projects enhanced [11]. Optimizing the antenna parts like the substrate thickness, patch, and feed line dimensions played a critical role on improving the antenna's characteristic. Apart from all these advantages, microstrip antennas showed a critical drawback and that was their narrow bandwidth (low fractional bandwidth (FBW = 7%)). To overcome this drawback, several researchers performed significant works over the last two decades. Various geometries have been introduced to satisfy the requirements of having a broad BW.

Some examples of most recent antennas to design with a wide BW are presented in this section. An antenna with a wide bandwidth (BW) and small dimensions along with an end-fire surface wave printed on a large metallic platform is also shown (Figure 1) [12]. The radiation pattern was improved at a higher frequency by a metasurface (MS) and blind-filled cylinder hole (BFCH) in the ground layer [13, 14]. Thus, the BFCH helped in maintaining the antenna dimensions small. Furthermore, to repress the TM_{01} mode propagation, any alteration on the reactance of MS array was effective. After antenna fabrication and measurement, the improvement on radiation characteristics at a higher frequency was obviously shown. In addition, an extremely wide BW of 3.78-18.54 GHz with a VSWR < 2.5 and high end-fire gain was obtained while the antenna dimensions remained small.

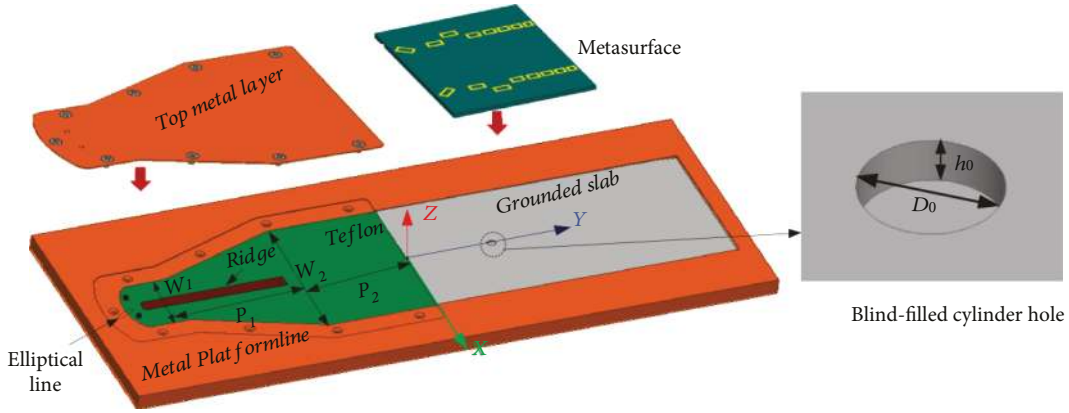

Figure 1: Wide bandwidth (BW) end-fire surface wave printed on a large metallic platform [12].

A Vivaldi antenna was designed to eliminate the cellular narrow band problem (Figure 2) [15]. Thus, the antenna covered most of the LTE bands 0.7-2.7 GHz. Unlike the conventional Vivaldi antenna [16] which uses a $\lambda/4$ open stub to feed the antenna, the proposed antenna was cut circularly with a $\lambda/4$ diameter [17] instead to make the antenna a traveling wave type and produce an end-fire radiation pattern. Therefore, it was designed and printed on a Rogers 5880 substrate with 0.508 mm thickness and dielectric constant of 2.2. The antenna was shortened to the ground using a shorting pin to act as an open stub with the length of a quarter wavelength. It was known that pins work better when they were connected at the edge; thus, it moved closer to the slot to attain better reflection coefficient results. Finally, two Vivaldi slots with an angle of 29 degrees were applied while the two pins shifted next to each other with coupling consideration between them. In addition, a rectangular slot separated two Vivaldi slots to improve the isolation.

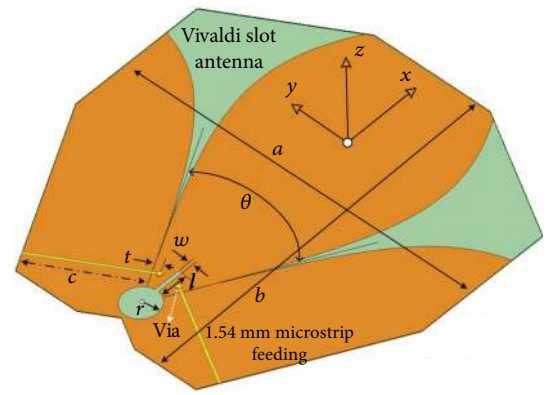

Figure 2: A Vivaldi antenna designed to eliminate the cellular narrow band problem [15].

The far-filled characteristics of the antenna were investigated for both in-phase and out-of-phase. Both efficiency and gain of the antenna were 7.4 dBi and 78% for in-phase and 4.05 dBi and 80% for out-of-phase. After the simulation, the antenna's characteristics were measured, and its performance was investigated.

A dual-mode planar inverted-F (type) antenna (PIFA) is designed to enhance the BW (Figure 3) [18]. By using the rectangular PIFA, all the even modes were ignored (to repress the even modes, the cavity model was used [19]). Afterwards, the proposed antenna was loaded by two vias to investigate how the odd modes varied and affected the results. In addition to the previous parts, the antenna had a shorting wall on one side of the rectangular patch and a narrow linear slot on the patch. It showed that parameters like radiating modes, vias, and width of the radiation patch assisted in enhancing the BW. After optimizing the PIFA antenna, the results illustrated that PIFA's BW was raised up to 15.3% along with two in-band resonances. As aforementioned, the proposed antenna's small dimensions were kept. Thus, it can be a good choice for many applications in which small dimensions matter such as military and satellite communications.

Another paper designed a dual-band PIFA antenna for the ISM band at both 433 MHz and 2 4 GHz (Figure 4) [20]. To achieve a wide BW, both the PIFA antenna and the ground layer were designed and simulated simultaneously without increasing the antenna's dimensions. At first, the first resonance (433 GHz) was achieved by the conventional PIFA, and then to resonate at the higher band (2.4 GHz), a slot was cut from the patch. In addition, the antenna was simulated and fabricated on a layer with a 6 mm height, 1.3 dielectric constant, and tanδ of 0.044. A textile layer considered as a metallic layer with conductivity of 1.18×10^5 S/m and thickness of 0.17 mm was pasted at the back with a glue. Then the patch, shorting wall, and ground fabricated on the textile substrate before it were fed by an SMA port from behind. The result showed that the radiation efficiency of the antenna dropped dramatically when it touches the body by almost 10%.

A circularly polarized (CP) dielectric resonator fed from only one terminal is presented in Figure 5 [21]. The proposed antenna comprised one rectangular and two half-split dielectric resonators with the shape of a cylinder. Moreover, the antenna was etched on a layer of the FR4 proxy with a permittivity of 4.4 and thickness of 0.8 mm. Moreover, a ground plane which consists of a rectangular slot was located at the top of the substrate and the two split cylinders surrounded the rectangular dielectric resonator (DR) symmetrically. All the DRs were made of ceramic materials with the permittivity of 12.8. In addition to that, all the DRs were chosen to operate

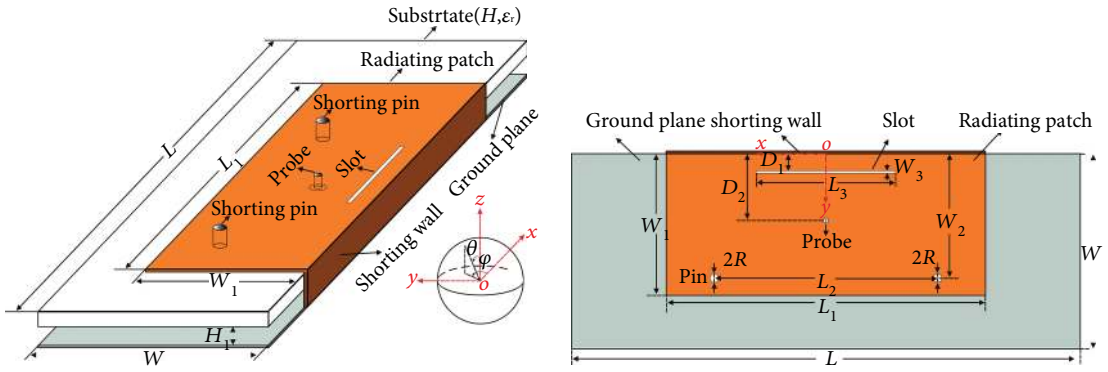

Figure 3: A dual-mode PIFA designed to enhance the BW [18].

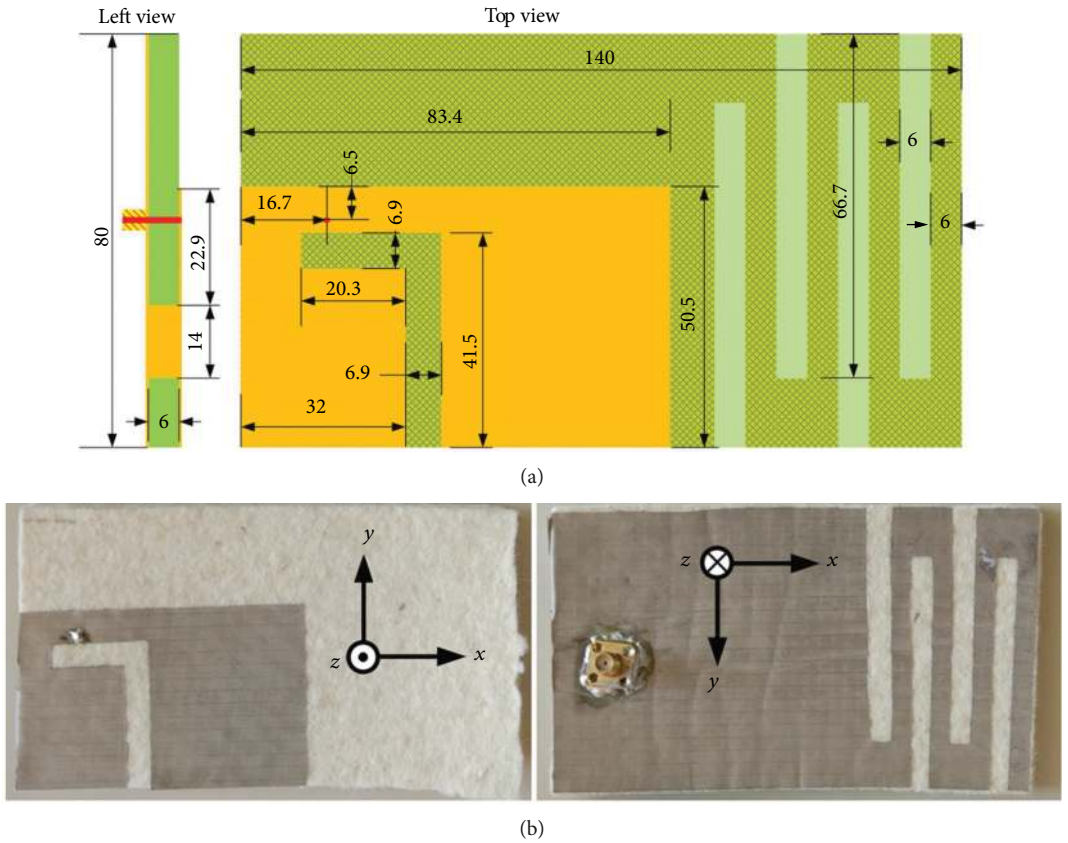

Figure 4: A dual-band PIFA antenna for the ISM band [20].

4.7 GHz for the fundamental mode of TE^{y}_{111}. To obtain the circular polarization (CP) radiations, two slots were cut from the orthogonal side to the main slot. This made the slot to have a shape like that of a stair. To achieve proper results for the antenna, the dimensions of the slots were optimized applying the high-frequency simulator according to the finite element method. The electric field was obtained at three different frequencies 4.75, 5.5, and 6.38 GHz with phase angle changes from 45° to -45° which gives 90-degree differences. Apart from the fundamental mode of TE^{y}_{111}, the other pairs of mode were investigated orthogonally such as TE^{x}_{121} and TE^{y}_{121} at 5.36 and 5.65 GHz and TE^{x}_{131} and TE^{y}_{131} at 6.27 and 6.57 GHz. The results showed that the impedance BW remained unchanged for both cases of the simulations, except the axial ratio (AR) which was altered dramatically as the AR became more than 15 dB for the rectangular slot, and it was kept below 3 dB when it changed to stair-shaped for a wider BW. Furthermore, the proposed DRA gave the impedance BW of 43.1% for a frequency range of 4.24-6.57 GHz when it was fed through the rectangular slot. Apart from that, the proposed CP DRA achieved the impedance BW of 46.9% and 49.67% for the frequency range of 4.2-

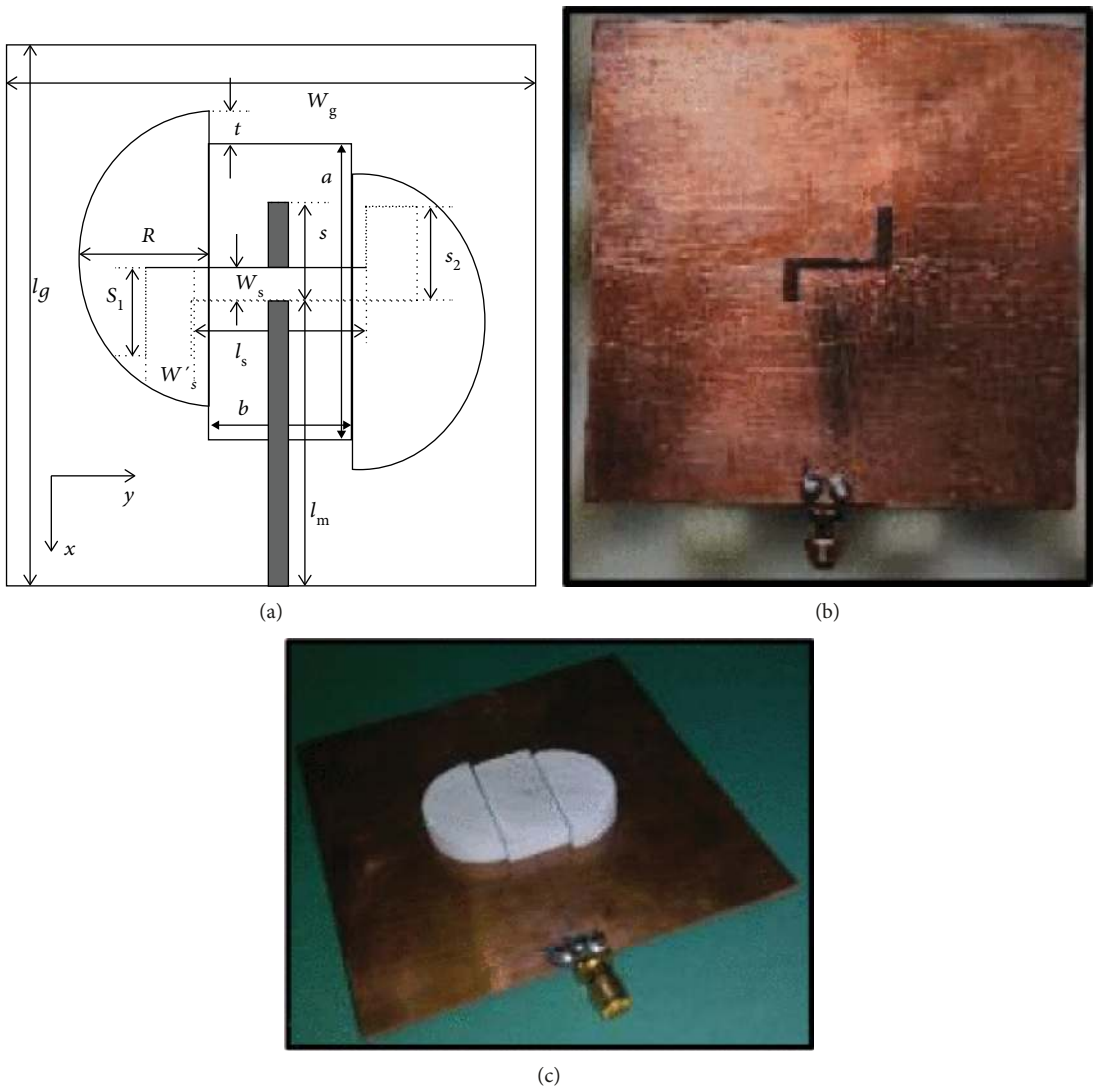

Figure 5: A circularly polarized (CP) single layer, and a single-feed planar slot antenna [21].

6.79 GHz and 4.1-6.81 GHz when it was excited through the stair-shaped slots. It was clearly shown that the radiation pattern was not changed and was stable throughout the frequency band and that both right-hand circular polarization (RHCP) and left-hand circular polarization (LHCP) radiation patterns were defined and drawn. However, RHCP showed a stronger radiation pattern by 20 dB. To show the performance of the proposed antenna, the antenna was optimized by checking the effects of displacement, ratios of the split cylinder, DR dimensions, side length, and slot length.

Therefore, the proposed antenna achieved an overlap BW with an acceptable AR and BW of 89% and 2.4-6.22 GHz, respectively, which made it applicable for UWB applications.

A mm-wave planar antenna with an end-fire radiation pattern in both E and H planes and acceptable impedance matching over the working BW (42.3-48.4 GHz) was presented for Q-band communications [22]. The antenna used a Rogers 5880 substrate with 2.2 permittivity, 0.0009 tanδ, and 0.508 mm height. Moreover, an angled umbrella-shaped dipole and three pairs of symmetrical directors were used to feed the antenna and all the directors had the same size, location, and tilting degree in both sides (Figure 6). Since the SIW was operating as a natural balun with independency of the frequency, the parallel strip lines were connected to the integrated waveguide technology (SIW) walls for feeding. Besides, the tilting angle of parallel strip lines was optimized to extend the beamwidth of the E-field. Based on the beamwidth electric field sensitivity of the antenna compared to the dipole tilting angle and directors' size, the SIW enabled the antenna in integrating with a planar circuit with minimum loss [23]. The antenna's return loss was below –12.5 dB all over the working BW and showed a good agreement between the fabrication and simulation results. The cross-polarization level was altered from -7 to 10 dB, and for higher frequency, it was able to be improved when a thinner substrate was applied [24]. Moreover, the antenna obtained a maximum measured gain of 5.2 dBi over the

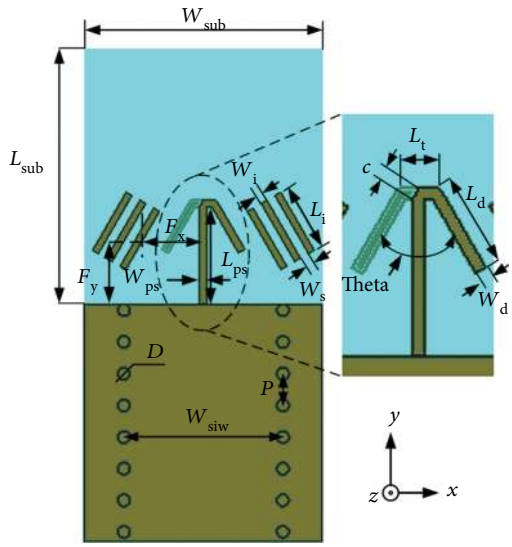

Figure 6: A mm-wave planar antenna with an end-fire radiation pattern in both E and H planes [22].

working BW, simulated gain of 5.5 dBi, and measured radiation efficiency around 82%.

A planar loop antenna achieved seven resonances to work for handset communication application frequency bands such as Global System for Mobile Communications (GSM) 850, 900, DCS1800, PCS1900, UMTS2100, and LTE2 300/2500 [25]. The proposed antenna had a small size ($60 \times 130\,mm^2$) designed and printed on a FR4 substrate $\varepsilon_r = 4.4$ and 0.02 tanδ and 0.7 mm thickness. Apart from the main system size of $60 \times 122\,mm^2$, a nongrounded part of $8 \times 60\,mm^2$ is located at the top side of the substrate. A stub was used to tune the impedance matching when it integrated with the system. In addition, the proposed antenna had a single loop connecting the feed point to the ground plane. Thus, to feed the antenna (considering the lowest resonant frequency while maintaining the antenna's dimensions), three meandering microstrip lines were integrated in both sides. Furthermore, to increase the BW at lower bands and create another resonance at 940 MHz, a "π" high-pass filter was used. Finally, to cover the other two bands GSM 850 and 900, a $\lambda/2$ loop was utilised. Afterwards, six modes of resonant occurred at the frequencies of 0.78, 0.915, 1.66, 2.04, 2.2, and 2.6 GHz. Hence, the attained working bands were GSM 850, 900, DCS, PCS, UMTS 2100, LTE 2300, and 2500.

A wideband monopole antenna with circular polarization (CP) which consisted of a 4×4 nonuniform H-shaped patch array was printed on the surface of a substrate with permittivity of 3.38 and thickness of 3.048 mm. The H-shaped cells were to improve the polarization effects. In each step of the design, the radiation modes were investigated to obtain proper excitation (Figure 7) [26]. Then, the final design was fabricated on three layers of substrate. The first two layers were RO4003 with the thickness of 1.524 mm which gave a total thickness of 3.034 mm. In addition to that, the third layer of RO4003 had the thickness of 0.813 mm. The antenna in [26] illustrated the impedance BW of 38.8% and a high cross-polarization rejection higher than 15 dB better than that presented in [27].

Another antenna with a tapered sickle slot shape cut from the crescent to create band rejections for an in-band WiMax frequency band (3.4– 3.69 GHz) with optimized dimensions of $57 \times 37.5 \times 0.8\,mm^3$ is a good choice for portable devices. The substrate used for both of these antennas was FR4 epoxy 0.8 mm thickness, $\varepsilon_r = 4.4$, and 0.017 tanδ. Moreover, both antennas had around 1 dBi gain variation and the max and min of the gain were 3.2 and 0.7 dBi, respectively. The proposed antenna's radiation pattern was measured, and it was noticed that it was stable at all the working bands.

Another wide-band loop antenna was designed for LTE (long-term evolution) and WWAN (wireless wide area network) of tablet PC [28]. The proposed antenna used a FR4 substrate, with 1.6 mm height, loss tangent of 0.02, and total size of $69 \times 10\,mm^2$. The proposed loop antenna was designed at the top and right corner of the GND layer with a size of $220 \times 130\,mm^2$. The proposed antenna had wide BW, low profile, and acceptable radiation efficiency. Due to the antenna's high performances, it can be integrated with an LCD of tablets and laptops. The antenna showed a stable and consistent radiation pattern over the working BW. The antenna fabrication method was fit for the printed circuit technology. Hence, it was a good candidate for LTE antennas used for transportable devices.

Some more researches have been done to design wide-band antennas for different applications, for instance, an IR UWB antenna with low complexity designed at a frequency band of 0–5 GHz with a less required silicon printed area [29]. The proposed antenna acted as a transmitter which employed RF/CMOS technology with a capability of signal control and BW tuning. Furthermore, the system utilised a very low printing area with an overall size of $0.024\,mm^2$ for the ASK modulation. In addition to that, the antenna had used a monopole antenna's working frequency bands of 1.5–3.7 GHz.

In another research, an electromagnetic band gap (EBG) structure was employed to create a broad pass-band and flat stop-band having a tapered shape and low profile [30]. Besides, to suppress the in-band ripples, a Chebyshev tapered shape was used. In addition to that, a defected ground structure (DGS) was applied to enhance the BW of the stop-band while keeping the EBG patterns' dimensions low. To attain higher attenuations and zeros of transmission, a spurline and open stubs were used. The proposed antenna demonstrated better performances in terms of low profile, flat pass-band, and broad pass-band compared to conventional EBG structures. Furthermore, the results indicated that the simulated design had a FBW of 93.7%. Some other wide-band antennas were presented in [31–33].

3. Wide-Band Monopole Antenna over a Metal Plate

Two antennas, a dual-band high-impedance surface structure along with a monopole antenna, were designed for the wireless local area network (WLAN) application. The

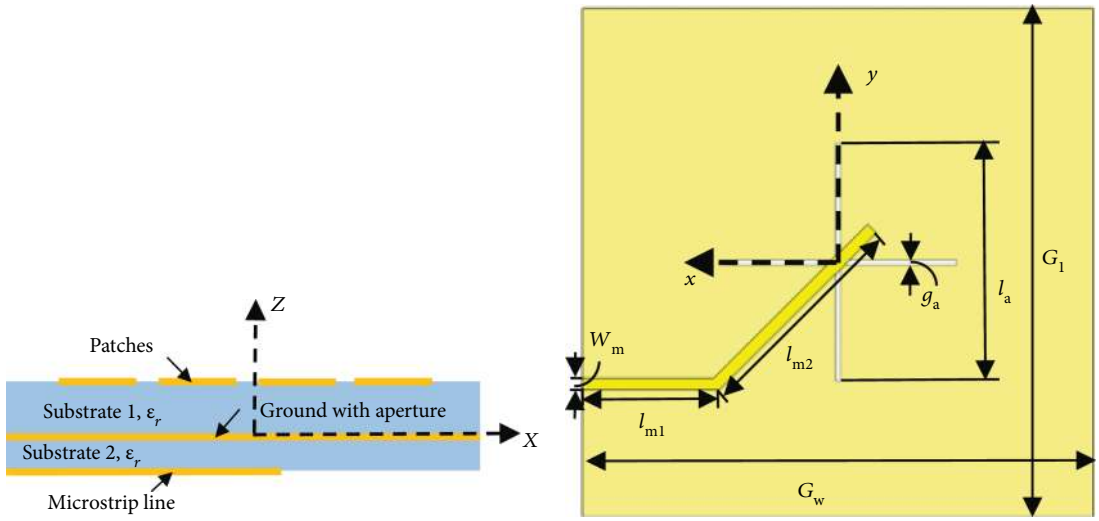

Figure 7: A CP monopole antenna with H-shaped cells on the first substrate [26].

operating frequencies for these antennas were 2.45 GHz and 5.25 (Figure 8) [34]. To design the antenna with high performances, some electromagnetic (EM) sheets such as metallic layers, R-cards, and high impedance surface (HIS) were exploited. The HIS was designed and simulated on the electromagnetic sheets initially to make two resonances at 2.45 GHz and 5.25 GHz [35, 36]. The proposed antenna had a fork-shaped resonator and a coplanar waveguide (CPW) feed line (50 Ω).

In addition, the antenna was fabricated on a FR4 layer with $\varepsilon_r = 4.4$ and 1.6 mm height. The HIS structure affected the reflection coefficient result negatively as it became worse over the working BW.

However, the antenna with HIS produced a wider BW at the working bands of WLAN. Unlike the reflection coefficient and BW, the forward radiations were not too much different between the antennas with and without HIS. But the backward radiations were dramatically decreased for antennas with HIS, and antennas' specific absorption rate (SAR) was reduced a lot as well. Hence, the proposed antenna was used to decrease the SAR due to its HIS structure and R-cards.

A monopole planar antenna with a metal plate and elliptical shape fed with different feedings was presented [37]. The monopole elliptical antenna was investigated in terms of reflection coefficient, directivity, and gain over the working BW. The proposed antenna was designed above the rectangular GND plane with dimensions of $300 \times 300\ \text{mm}^2$. Both the plate and single feed were integrated together. Afterward, the feeding strip's dimensions were optimized to get the perfect match. This perfect matching benefitted us with a broad BW from 1 GHz to 14 GHz. In addition, when the feed line was 1.5 mm, the BW of 6 GHz was achieved and when it was 2 mm, 4 GHz BW was achieved. Besides, different lengths of the feeding line showed varied amounts of gain. For example, when it was 1 mm, 1.5 mm, and 2 mm, the gain became 6.11, 6.01, and 6.04 dB, respectively. The same trend went for the directivity as it was 5.88, 5.79, and 5.82 dBi, respectively. Hence, it depicted that when the length was 1 mm the BW was illustrated to be the widest and the antenna was able to be applied for UWB applications.

Another metal-plate monopole antenna was designed for indoor communications like digital TVs (DTVs) which covered the ultra high-frequency (UHF) band [38]. The antenna consisted of a rectangular-shaped patch and a square ground plane along with a gap. In addition to that, the antenna was fed by an SMA (subminiature version A connector) port from behind the antenna. To have a wider BW, some parameters like monopole antenna dimensions, feeding gap, and GND size were optimized [39]. Moreover, the complete explanation of bevel angle effects on the antenna performances is presented in [40]. In addition to that, the GND size had impacts on the reflection coefficient result as a smaller size of the GND layer enhanced the lower edge of the lower frequency band. It was seen that the antenna obtained an omnidirectional radiation pattern with a low level of cross-polarization.

A trident-shaped antenna was mounted on a square metal plate with a ground plane size of $150 \times 150\ \text{mm}^2$ (Figure 9) [41]. The proposed antenna used only a single plate for fabrication and was then fed by the feeding lines. In addition, the trident-shaped antenna was fed by the feeding strip attached to the central branch and then two side branches were spaced by a t distance from each other. These two side branches had the same shape and wide impedance BW obtained by optimizing them. The total dimensions of the proposed square monopole antenna were $40 \times 40\ \text{mm}^2$ which assisted in having a wide BW over the band and a low-frequency edge lower than 2 GHz. Besides, by optimizing and adjusting the effective parameters such as t, h, and d, the upper end of the working frequency band was attained to be more than 11 GHz. The measured result showed a promising 10 GHz BW from 1.376 to 11.448 GHz. Hence, the achieved wide BW proved that the antenna was a

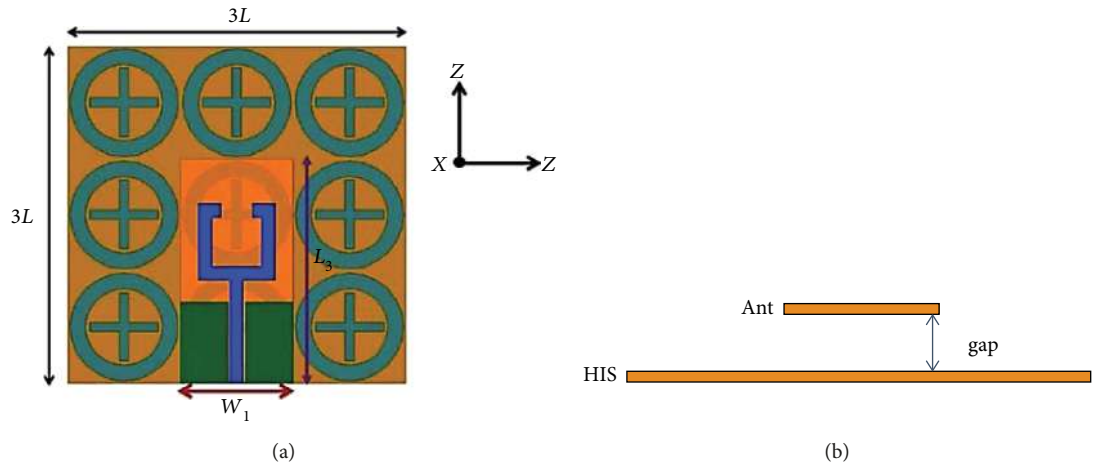

Figure 8: Two antennas, a dual-band high-impedance surface structure along with a monopole antenna [34].

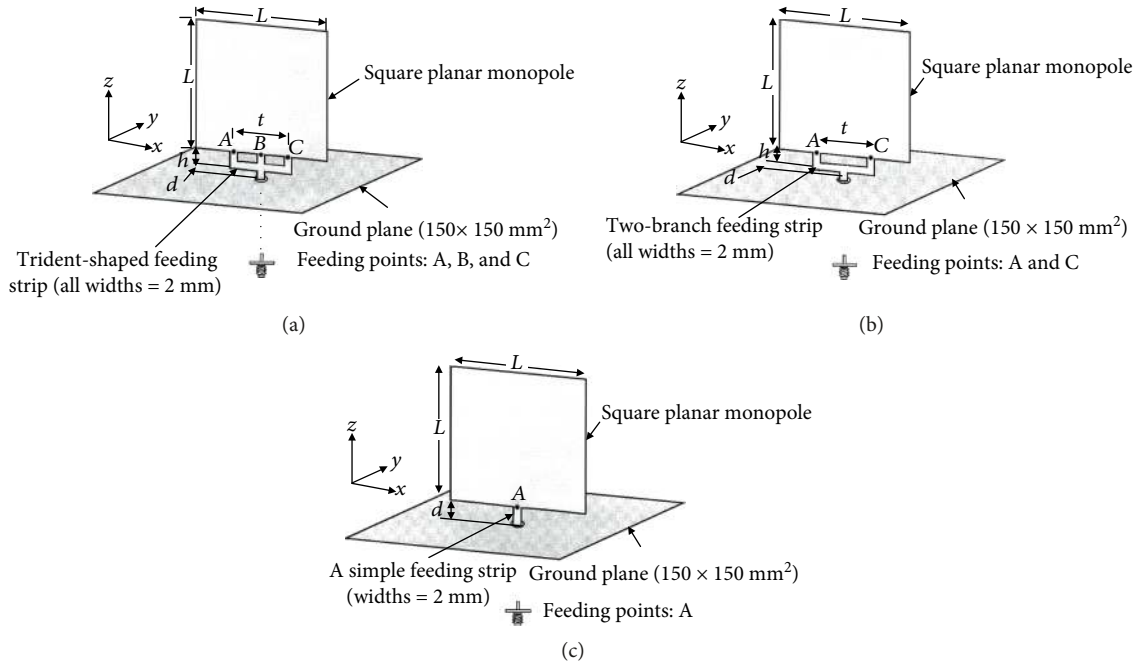

Figure 9: A trident-shaped antenna mounted on a square metal plate [41].

promising choice for broadband antennas using the IEEE 802.16a (2–11 GHz) standard.

In optimizing the antenna dimensions to get the maximum possible gain, it was observed that the plate width affected the antenna gain. Thus, it showed that the antenna had an increase in gain for lower frequencies up to 6 GHz (4.0 to 7.0 dBi), and this variation increased slightly for higher frequencies from 6.5 to 7.0 dBi. Moreover, it was depicted that parameter d had too much effect on impedance matching as the achieved wide BW for higher frequencies when it was 1 mm.

A monopole antenna with a shape of square cylindrical was simulated and fabricated on a cross-shaped metal plate to be used for applications that needed a wideband with an omnidirectional radiation pattern [42]. The square GND plane dimensions were $120 \times 120\,\text{mm}^2$, and the antenna was mounted at the centre of this plate with a feed gap of 2 mm. In addition to that, the antenna printed area was small with $8 \times 8\,\text{mm}^2$ cross section and 28 mm length and the antenna achieved a wide BW of 7.5 GHz from 1.855 to 9.415 GHz. Since the proposed antenna was symmetrical, thus an omnidirectional pattern was expected [43]. The antenna has a similar trend with another research in terms of the planar square shape and two notches cut from the antenna to improve the BW [44]. It was observed that both simulated and measured results were in good agreement. It was clearly shown that the antenna obtained 7.5 GHz BW to cover the IEEE 802.16e standard (2–6 GHz). Finally, the proposed antenna demonstrated a good and applicable omnidirectional radiation pattern.

To obtain a minimum return loss, an antenna with a planar structure and UWB BW was presented [45]. The antenna dimensions and the other design parameters were optimized to achieve an antenna with high performances. To obtain the best and optimized values for the parameters, simulated annealing (SA) was used. Then, the finite element model (FEM) technique was utilised for segmentation and analysis [46]. To reduce the computation time and accelerate the process time, a semi-sphere was used instead of a complete one. Furthermore, the proposed antenna consisted of two copper plates, one for the ground plane and the other for the antenna itself. The antenna was fed through an SMA port from behind, and the monopole antenna was soldered to the GND plane (10 cm) and a little gap considered between them. It was observed that the radiation pattern of the antenna for $\theta = \pm 90^{\circ}$ remained stable. Apart from the radiation pattern, the proposed antenna achieved excellent return losses (<10 dB) with broad BW 2-20 GHz; hence, the proposed UWB antenna was a promising choice for UWB applications.

4. Wide-Slot UWB Antennas

To obtain a wide BW, many types of antennas like spirals, log periodic, and tapered were used [47]. A planar antenna suitable phased array application was designed here. It consisted of a circular ring patch with inner and outer radii of $r_1 = 4.5$ mm and $r_2 = 9$ mm, respectively, and then fed by a microstrip line. The total dimensions of the antenna were 42 mm × 50 mm × 9 mm. A coupled *S*-shaped strip was printed behind the antenna to attain a voltage standing wave ratio (VSWR) < 2.5. In addition, to have a unidirectional antenna, an absorber was used along with the GND layer. Both antennas were fabricated on a substrate with $\varepsilon_r = 2.2$ and $h = 1.6$ mm. An acceptable VSWR was achieved over the working BW from 6 GHz to 18 GHz for both unidirectional and bidirectional antennas. Moreover, the maximum gain was varied from 1.3 to 3.6 dB for the bidirectional antenna and -2.5 to 1.5 for the unidirectional antenna over the working BW. Thus, the proposed antenna was used for communication applications and electronic warfare (EW) antenna arrays.

A shape-blending algorithm was used to design an antenna with a wide slot to have a wide BW (Figure 10) [48]. The proposed antenna comprised a wide rectangular shape slot and a stub for tuning and then fed by a CPW feed line. The proposed antenna was mounted on a substrate with $\varepsilon_r = 2.2$ and 0.787 mm height and loss tangent of 0.0009.

The return loss result of the antenna was mostly suffered by the tuning stub's dimensions and shape. Other parameters like the width *W* affected the impedance matching. In addition, the tuning stub shape was dependent on the blending coefficient *t* as it increased the BW. To validate and check the antenna performances, six prototypes of the slot antenna were fabricated and measured by varying the stub shape. The proposed antenna showed an omnidirectional radiation in the H plane. However, this pattern changed to bidirectional in the E plane. In addition, the measured and simulated impedance BWs were 126.4% and 138%, respectively. Due to the low profile and simple structure, it was a promising structure for wide-band applications.

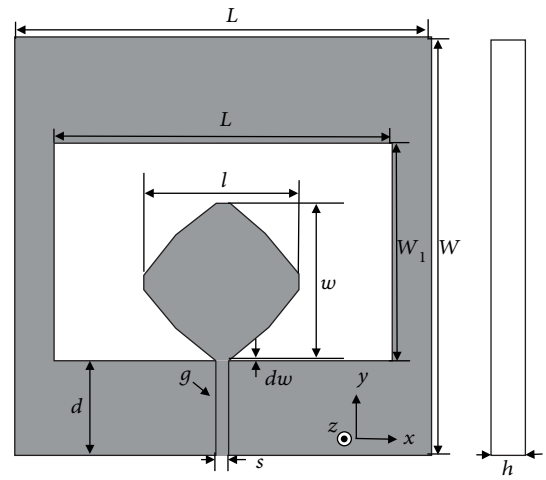

Figure 10: A shape-blending algorithm was used to design an antenna with a wide slot [48].

Another wide-slot microstrip antenna was designed for UWB applications (Figure 11) [49]. The proposed antenna was simulated and printed on a layer with $\varepsilon_r = 2.65$ and 1 mm height. The antenna comprised three slots, one elliptical and two circular located at the bottom of the substrate. These slots produce new current paths.

Furthermore, they were assumed as tools for better impedance matching and antenna dimension reduction. A circular patch located on top of the substrate and above the elliptical slot was used to increase the BW by coupling with them. To improve the BW further, two semicircular slots and four quasitriangular slots were cut from the patch. All the dimensions and values were optimized to get the best values. The result illustrated that the slot with an elliptical shape has large effects on the low-frequency edge. However, more added slots reduced the low frequency. Thus, the antenna dimensions were too large without the slots as 400×400 mm^2. After measurement, a wide BW in the range of 0.34 GHz to 10.28 GHz was achieved. Furthermore, the antenna had almost an omni-pattern in the E plane and bidirectional pattern in the H plane at low frequency. When the frequency was enhanced, the electrical length of the antenna increased and so did the nulls in patterns. In addition to that, the radiation pattern of the antenna was symmetric and stable over the working BW and it was bidirectional at low frequency and omnidirectional at high frequency. Hence, the proposed antenna was a promising device for UWB applications.

A circular slot antenna was fed by the CPW method to have tunable dual-band notches along with frequency reconfigurable properties. Then, its characteristics were verified by fabrication and measurement to show that it was applicable for UWB applications [50]. The antenna comprised a circular resonator, a circular slot, and a CPW feeding. Moreover, the antenna was simulated on a layer with $\varepsilon_r = 2.65$ and $h = 1.5$ mm thickness. Afterward, the *T*-shaped stepped impedance resonator (T-SIR) or the parallel stub-loaded resonator

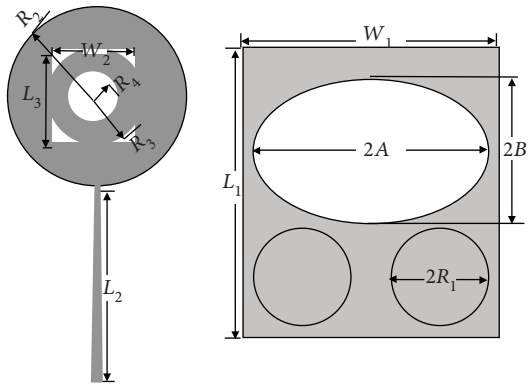

Figure 11: A wide slot microstrip antenna with three slots, one elliptical and two circular [49].

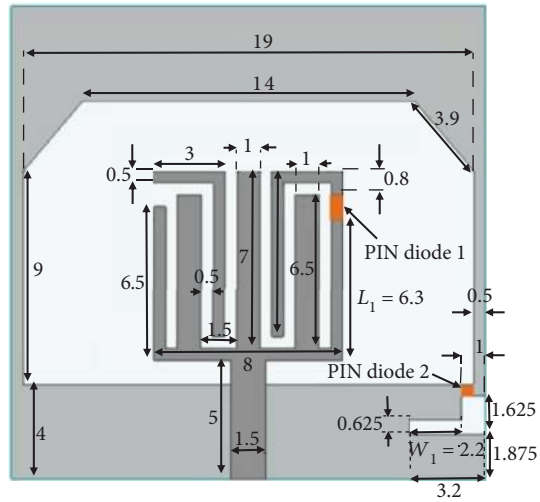

Figure 12: A microstrip slot antenna with the ability of reconfigurable frequency along with switchable band notches for an ultra-wideband [56].

(PSLR) were employed to get the band notch characteristics. Both the T-SIR and the PSLR were employed at the same time to obtain the two stop bands. In addition, to obtain the configurability of the antenna, three switches named SW1, SW2, and SW3 were used. Using TSIR, 5.5 GHz WLAN was given and PSLR gave a notch band at 8 GHz. To apply these switches, a metal bridge showed the on-state and off-state when it is not implemented [51–54]. Hence, implementations of the switches helped to attain the ultra-wide BW operating from 2 7 GHz to 12 GHz. Furthermore, the proposed antenna had a monopole antenna's omnidirectional radiation pattern in both E plane and H plane. Thus, the antenna was suitable for UWB applications.

A circularly polarized (CP) slot antenna with an elliptical shape fed by CPW presented in [55] was used for UWB applications. The designing procedure started with a design of the conventional elliptical patch antenna fed by CPW. After optimization of the antenna, the overall dimension of the antenna became $40 \times 40\,\text{mm}^2$. The antenna mounted on an epoxy FR4 layer has $\varepsilon_r = 4.4$, 0.025 loss tangent, and 1.59 mm thickness. The antenna got 6.66 GHz impedance BW for 3.67-10.33 GHz. But the antenna's gain was too low at this stage as 1.2 dBi. To improve the antenna performances, the conventional patch converted to a planar slot antenna which patch acted as a widened tuning stab. After converting, a band notch occurred from 3.66 GHz to 5.53 GHz. To obtain a CP characteristic, two stubs with the shape of a triangle were used at both the lower and upper right corners of the slot. The proposed CPW-feed printed slot antenna's working BW improved to almost 9.88 GHz and 136% FBW. Furthermore, the antenna's maximum gain improved as well to 4.31 dBi at 4.45 GHz. The antenna got the same radiated power in forward and backward directions, and the antenna proved that it was useful for UWB application along with WLAN/worldwide interoperability for microwave access (WiMax) applications.

A microstrip slot antenna which had the ability of reconfigurable frequency along with switchable band notches for ultra-wideband applications was designed and fabricated (Figure 12) [56]. The proposed antenna printed on both sides of a cheap FR4 layer was used with 0.8 mm height, tanδ of 0.018, and permittivity of 4.4. Furthermore, the antenna comprised a modified square-shaped and L-shaped slot cut from the GND layer and a feeding line. Two PINs were applied to attain the frequency reconfigurable ability which connected the patch to the GND. In addition to that, the antenna was switchable for four states. For further improvement, the square patch was converted to a fork-shaped patch along with two trips with the shape of a triangle over the working BW of 3-13.6 GHz. Besides, the two inverted L-shaped strips created a band rejection at 4.51-5.7 GHz. Thereafter, the L-shaped slot was utilised to eliminate the band rejections just created. The proposed antenna obtained a BW of 3.8-13.5 GHz. Thus, the proposed UWB antenna was able to be used for the WiMax band. The obtained BW was achievable only when both of the diodes on otherwise band notches would be occurred. The antenna attained a dipole-like and omnidirectional radiation pattern E and H plane, respectively [57]. Therefore, the proposed antenna had no complex configuration and low profile, suitable in a variety of wireless systems.

Another simple-structure, low-profile, low-cost antenna was designed for UWB application [58]. The antenna consisted of a tapered microstrip feed line and a ring-shaped monopole. The antenna was printed on a layer of Rogers 5880 with $\varepsilon_r = 2.2$ and $h = 0.787$ mm. Besides, the antenna had a maximum size of $16 \times 12 \times 0.787\,\text{mm}^3$. For further improvement on the BW, the conventional microstrip feed line converted to a tapered microstrip feed line as BW enhanced up to 25 GHz. Although there were more techniques for feeding the antenna, the tapered method was used due to its simplicity and better performances. The antenna showed a simulated wide BW from 6.5 GHz up to 25 GHz. Furthermore, the measured results illustrated the working BW of 1-13.5 GHz. Omnidirectional and bidirectional patterns were achieved in the H and E planes, respectively, and the antenna demonstrated a gain of 2-2.9 dBi in the frequency range of 6-22 GHz. Based on the results, the antenna

presented an acceptable radiation pattern and BW needed for UWB applications.

A compact antenna with characteristics of two band notches fed by the CPW technique is presented in [59]. To reduce the interference of the antenna, two U-shaped slots and one rectangular slot were applied to obtain the characteristics of band notch function through CPW feeding. Then, the antenna became suitable for UWB application except two working bands of 5-6 GHz and 7.7-8.5 GHz for the X-band. It was printed on a layer with $\varepsilon_r = 2.65$, $\tan\delta = 0.002$, and 1.6 mm height. In addition to that, the antenna had total dimensions of $21 \times 28\,\text{mm}^2$. When the patch resonator's dimensions were increased, the band notch at a higher band was removed and the notch at the lower band shifted slightly. Moreover, the omnidirectional and quasi-omnidirectional patterns were achieved on the $x-y$ plane and $x-z$ plane, respectively, and it was stable over the working BW as compared to wire dipole antennas.

5. Stacked Patch Antenna

Since the time delay responses were important in designing UWB antennas, a new method of designing small-sized circularly polarized (CP) slot antenna was presented [60]. The proposed antenna arrays were designed with considerations of focal distance in the aperture's diameters. Furthermore, the trade-off between the spillover loss and aperture efficiency was assumed. The spillover loss was reduced when aperture f/D decreased while the aperture efficiency was acceptable. The design procedure was divided into zones which was identical. First, the aperture was calculated. Then, the other parameters such as unit cell dimensions, permittivity, substrate loss tangent, and patch size and number came into consideration. After fabrication, the proposed TTD miniaturized-element frequency selective surface- (MEFSS-) based CP reflect array was experimentally characterized and investigated. The proposed antenna was operated at the X-band, and it provided a wide band and a true time delay over 40% of BW. When the antenna was fed by an offset version, it provided right-hand circular polarization (RHCP) beams for a maximum direction of 45 degrees. In addition, the antenna got the fidelity factor more than 91% for BW higher than 40%.

A stacked patch antenna was designed with a small size for UWB purposes [61]. When a patch was fed by the coaxial line, its BW decreased due to the high Q-factor. It was known that when the substrate thickness increased, the Q-factor reduced and the BW enhanced. When the coaxial length did not increase, the folded-patch feed technique was applied to solve the quality (Q) factor problem [62]. The stacked antenna comprised a patch with a T shape, a shorting wall ($7.5 \times 10\,\text{mm}^2$, able to reduce the overall size), a GND layer, and a folded patch feed with an angle of 35 degrees. In addition, the antenna's dimensions were $15 \times 17 \times 10\,\text{mm}^3$ printed at the centre of the GND layer with dimensions of $60 \times 60\,\text{mm}^2$. In the design procedures, a thick antenna with a height of 10 mm was used, but the probe length was only 3 mm. The T shape and the patch dimensions were optimized to get the highest performances of the antenna. The antenna showed a measured BW of 107.46% and simulated BW of 107.25%. Furthermore, the proposed antenna presented more improvement as compared to the conventional folded one and got smaller dimensions compared to some other articles. Then the antenna was measured and the gain showed a gradual increase to 5.8 dBi at 7.5 GHz, and after that it started reducing. The proposed antenna radiation pattern made it applicable for indoor wireless communications.

A folded patch fed stack antenna was presented for UWB applications [63]. The patch located at the centre of a GND layer with dimensions of $80 \times 80\,\text{mm}^2$ and a shorting wall made of copper connected the upper patch to the GND layer to decrease the antenna dimensions and increase the impedance BW. The simulated VSWR was in the range of 3.47–10.14 GHz, and the measured one was 3.75–9.86 GHz (90%). In addition, it obtained 90% FBW with dimensions of $15 \times 15 \times 10\,\text{mm}^3$ and maximum gain of 4.36 dBi attained in the $x-z$ plane over the frequency band. Therefore, the antenna was capable of working for UWB applications.

A UWB antenna with a wide slot was presented to be used for a populated static array developed at Bristol University for breast cancer detection [64, 65]. A wide-slot antenna fed by a fork-shaped resonator was replaced with the previous antenna. Then it was printed on a substrate with permittivity of 10.2. This permittivity was used due to a reduction in the interference caused by the permittivity difference of tissue and the antenna's substrate. Furthermore, the antenna which was a slot fed by the microstrip line was used to ignore the inductance caused by the coaxial probe. The patch layers became sandwiched to achieve the lower end of the UWB antenna. After using the finite-difference time-domain (FDTD) analysis of the proposed antenna, the antenna attained radiation efficiencies of 88%, 97%, and 97% at 4 GHz and 97% at both 6 and 8 GHz, respectively. The forked microstrip feed line splits the impedance of 50 Ω to 100 Ω. Furthermore, the fork feed and some cavities used consisted of an absorber line and a brass enclosure to extend the operating BW. The antenna achieved radiation efficiencies of 60%, 80%, and 90% at 3 GHz, 6 GHz, and 9 GHz, respectively, along with an impedance BW from almost 4 GHz to 10 GHz which was adequate for UWB applications. In addition to that, the antenna got acceptable time domain characteristics like low distortion over the BW. However, the antennas got the same amount of the gain, but the directivity of antenna with a wide slot was slightly different. Eventually, the wide-slot antenna performed well over the entire frequency band. Thus, the wide slot antenna was a promising case for UWB communications and the result confirmed that.

A rectangular microstrip patched stack antenna was cut by a U-shaped slot along with another patch with different dimensions printed on a separated layer presented in [66], and then its characteristics were investigated. In addition to that, the antenna fed through a coaxial probe was used due to its low spurious radiations and it was known as one of the popular techniques. The quasi-Newton was used to optimize the patch and the transmission line dimensions to achieve the perfect matching between the feed line and the patch. Furthermore, the antenna comprised two layers of dielectric with dimensions of $90 \times 80\,\text{mm}^2$ as the underneath

layer's patch and the upper layer had dimensions of $39.4 \times 29.4\,\text{mm}^2$ and $26.5 \times 18\,\text{mm}^2$, respectively. After optimizing the antenna and patch dimensions, the *U*-shaped slot was cut from the patch to affect the coupling between the slots. As increasing lot dimensions enhanced the coupling, so did the overall impedance matching. Therefore, the *U*-shaped slot controlled the coupling. Both substrate and the GND layer had the same dimensions. To characterize the probe feeding technique, a Gaussian pulse was used for UWB transmission in frequency 3-10 GHz [66]. Then a slot was applied to cover the BW partially for the frequency range of 3.60–5.44 GHz. The reflection coefficient result showed two resonances, one for the slot and the other one for the upper patch. However, the top patch's width controlled the higher resonance frequency while the *U*-slot affected both the lower patch and the resonance. To attain a wider BW, some parameters such as *U*-slot dimensions, position of the feeding point, and probe radius were optimized. The antenna achieved a cross-polarization magnitude level of 16 dB, a wide beamwidth of 108 degrees in the E plane, a wider BW of 56.8%, and a directional pattern over the frequency range. Hence, the antenna was suitable for UWB applications which needed a directional pattern.

6. Taper Slot UWB Antenna

A linear tapered slot Vivaldi antenna altered the appropriate dimensions on the edge to adjust the mutual coupling (Figure 13) [67]. The proposed antenna had a copper layer with the thickness of 0.017 mm at both sides, printed on a substrate of Roger TTM3 with the permittivity of 3.27 and 0.3807 mm thickness and nil tangent loss. The antenna consisted of a slot cut from one side of the antenna on a substrate layer. The taper slot was for high-frequency matching initially, and the wide end of it was for the lower-frequency matching.

Furthermore, the taper shape was a compound of three lines: one for high frequency and the other two for the linear low frequency. When the linear lines increased, the taper slot got an exponential shape and the beam became narrower, and when the arrays were corrugated, the coupling reduced [68]. The antenna achieved a maximum length of 72.92 mm at a cutoff frequency of 3 GHz. Moreover, it achieved VSWR < 2 over the working band of 3.1-20 GHz. Furthermore, the proposed antenna had a FBW of 146% over the operating band. Besides, the tapered slot antenna was able to receive signals from one direction and a good agreement was achieved between the beamwidth and the side lobe of the antenna. The antenna proved that it was applicable for UWB applications and it was able of integrating simply with circuits.

Another tapered slot antenna was designed for UWB communications [69]. Due to the dimensional tolerance and its infinite BW, the taper slot antenna was fabricated. The antenna's BW increased by optimizing the physical dimensions of the radiator. Besides, by cutting rectangular slits from the radiator, the impedance BW improved and the printed area of the antenna reduced by 15.5%. The antenna was fabricated on a FR4 layer with $\varepsilon_r = 4.7$, tan δ of 0.019, and 1.6 mm thickness [70]. The impedance BW of the antenna met the UWB requirements of having VSWR < 2 for frequency bands of 2.33-6.46 GHz and 8.84-11.32 GHz. After inserting the rectangular slits, the antenna obtained an impedance BW of 3.64-10.84. Moreover, stable matching characteristics were achieved after the slits were used. In addition to that, structure 1 got 3.26-6.99 GHz and the second structure attained a BW of 3.55-12 GHz. When both the simulation and measurement results were in good agreement, the antenna's pattern analysis was started in both planes. At 3 GHz, the beamwidths were 130 degrees and 77 degrees in the E and H planes. The first structure had a 3 dB beamwidth of 85° and 77° at 4 GHz and 78° and 65° at 5 GHz in the E and H planes. Moreover, the second one had a beamwidth of 140° and 75° at 3 GHz, 95° and 110° at 4 GHz, 84° and 64° at 5 GHz, 62° and 55° at 6 GHz, 55° and 68° at 7 GHz, 42° and 90° 8 GHz, and 41° and 85° at 9 GHz in the E and H planes, respectively. Therefore, the first antenna got a wider BW. The total printed area of the antenna was $4200\,\text{mm}^2$ for the first structure and $3550\,\text{mm}^2$ for the second one. After analysis, the antenna proved that it had the ability to work for location recognition.

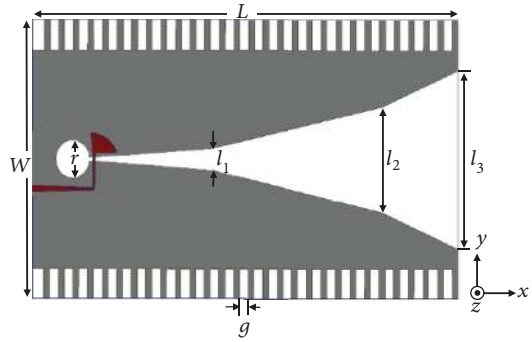

Figure 13: A linear tapered slot Vivaldi antenna [67].

A quarter-wave Chebyshev transformer was applied to get the impulse responses and performances of a UWB taper slot antenna [71]. The presented tapered slot antenna was fed by a transmission line, and the BW was restricted due to the following reasons: the microstrip feed line, the cavity termination made at the back, the antenna dimensions, and the taper slot. To attain a wider BW, a Chebyshev mathematical approach was used to make a model of the slot line and smooth the design steps. The transformer was designed for maximum possible reflection coefficients. Besides, it gave equal pass-band ripples in the working band. The antenna's radiation characteristics and E-field components for both polarization were considered. It was obvious that the transmitted pulse was changed along with its parameters such as peak value, pulse width, and ringing value. Moreover, the antenna showed a good performance with low distortion in the 3 dB half-power beam and maximum peak obtained to design the CS points for the cubic line and the outer CS points. However, the exponential shape got a better peak compared to cubic spline because of more gain in the frequency domain, and the taper design with a cubic spline got a lower ringing [72]. The proposed technique in this research had the benefit of helping in optimizing the antenna

to get a reflection coefficient result and obtain a low-profile antenna. In addition, it was concluded that the antenna presented here was suitable for UWB applications since it attained the highest amplitude, narrowest pulse width, lowest phase distortion, and minimum ringing.

A new Vivaldi antenna design was used using stepped connections between the slot and the tapered patch [73]. The proposed printed antenna was mounted on a FR4 layer 0.8 mm height [74]. Besides, the proposed antenna used a slot line transition structure for excitation along with two exponential tapered shapes. These exponential shapes were connected to the slot lines at both sides of it. Furthermore, the stepped shape was used for better matching. After cutting the slot line as the stepped lines, a perfect match occurred between feed and lines when the gap was optimized. The proposed antenna attained a broad BW of 3.1-15 GHz with VSWR < 2. Thus, the proposed antenna became suitable for UWB applications. In addition to that, the antenna obtained a maximum gain of 5.1 dBi at 5 GHz and 8.2 GHz at 9.2 GHz and it achieved a radiation efficiency of 70%. Furthermore, the antenna had a stable unidirectional radiation pattern in both E and H planes and an end-fire main lobe in the y -direction. Besides, the 1.3 ns group time delay with the tolerance of 0.5 was obtained at the main direction of the antenna. It was clearly noticed that both simulation and measurement results were in good agreement.

Another tapered slot antenna fed by CPW with notch bands was proposed for UWB applications [75]. First, a monopole-type antenna UWB antenna with a single end called antenna A was designed; it was comprised of a circular patch and a tapered-slot GND. Then, it was fed through the tapered slot which made many resonances and more modes. Afterward, to improve the matching, a rectangular slot was cut from the circular patch. Furthermore, antenna A had the size of $30 \times 28\,\text{mm}^2$ and the working BW of 2.86-12.4 GHz. On the other hand, antenna B used a symmetrical circular slot along with a differential tapered slot. These circular patches were connected through CPW feed lines. Antenna B got a size of $30 \times 35\,\text{mm}^2$. In addition, antenna C got sharp notch bands when two open-ended stubs were put inside the tapered slot GND symmetrically, and then two slits were printed on two patches with symmetrical circles. Both antenna A and antenna B obtained a very low cross-polarization in the H plane, and antenna C achieved a BW of 2.27-12.3 GHz along with the band notches in BW. The proposed antennas achieved an H plane omnidirectional radiation. Since both the simulated and measured results were in good agreement, it proved that it was a good choice for UWB applications.

A new design of tapered slot antenna with a shape of antipodal was designed [76]. The antenna was printed on an FR4 substrate with a 1 mm height and then fed by a transmission line for more impedance matching. However, this feed line was considered as balun. In addition to that, it was connected to large and curvy fins to improve the reflection coefficient results and the tapered angle was optimized to get a better directivity [77]. Then, to obtain better antenna characteristics, the fins were folded. These fins increased the surface current and more resonances. Furthermore, when the substrate thickness increased, the reflection coefficient results reduced from 1 to 4 GHz. It was noticed that the folded TSA attained fewer reflection coefficient results than did the conventional TSA especially at lower bands. Due to the acceptable results such as wide BW 1-11 GHz, uninfluential group delay, and lower back radiation pattern, the proposed TSA antenna was a good choice for UWB applications.

Another exponential-shaped TSA with a late time ring was designed for UWB applications [78]. The antenna was printed on a FR4 plate with ε_r and height of 4.4 and 1 mm, respectively. The antenna became more compact after cutting two corners of it. The antenna was assumed as a mixture of both electronic resonator (ER) and magnetic resonator (MR) because of having tapered lines, arc 2 and slot 1, and MR for having the loop which contained arc 1 and slot 2. In addition, the MR impacts were considered by the current distributions. The two resistive elements connected the loop to the ground through vias. Then, a five-section Chebyshev transformer was used to have better impedance matching. Finally, it was fed through a microstrip line and the width of this line was optimized for a wider BW. Although the antenna was bended to a quarter, still the dimensions were $200 \times 170\,\text{mm}^2$. The antenna attained a working impedance BW of 0.65-6 GHz with VSWR < 2. Moreover, the antenna's radiation pattern was like a dipole antenna's radiation pattern in both E and H planes and it achieved a stable gain of 3 dBi for higher frequency and the maximum gain of 8 dBi at 5.5 GHz. Hence, the antenna assumed to be a good candidate for radar systems or wireless communication systems due to its low-profile dimensions.

A high gain, wide BW, and end-fire radiation pattern TSA Vivaldi antenna were presented in [79]. The proposed antenna consisted of an aperture with 8 degrees on one side and then fed through two tapered lines by a 50 Ω SMA port. Furthermore, the antenna was mounted on a Rogers 4003 layer with dielectric constant of 3.55, tan δ of 0.0018, and 0.8 mm thickness and the final dimensions of the antenna as $100 \times 60\,\text{mm}^2$. The antenna operated in a wide BW from 6 GHz to 18 GHz with VSWR < 2. The applied aperture improved and increased the radiation efficiency at higher frequencies. Therefore, when they opened the aperture, the operating BW of 6-18 GHz started covering from 2.99 to 23.6 GHz. However, the applied method in this paper decreased the ripples and the picks of the reflection coefficient result of the antenna, and it showed an increase in cross-polarization level. Hence, the new model was utilised to decrease the side lobe level (SLL) and the antenna's front/-back ratio and obtained a symmetric BW in both E and H planes. Thus, the antenna with these fantastic characteristics was applied for UWB applications.

A Y-shaped TSA antenna with corrugated edges was designed with enhanced BW [80]. The antenna was designed on a substrate with dimensions of $145 \times 80 \times 1\,\text{mm}^3$. Then, the antenna gain was enhanced by using two slots as compared to the single one. Afterward, these two slots were separated by a V-shaped metal surface to improve the directivity of the antenna. Furthermore, it reduced the power at higher modes, the surface current extended when the Y-shape was applied, and the exponential curve was used next to the

Y-shape corrugated to focus the energy. In addition, a direct short-circuit method was applied to widen the BW and ignore the surface waves especially at higher frequencies. As a result, the working impedance BW of the antenna was from 2.5 to 28 GHz, the antenna's gain was bigger than 10 dB from 3.5 GHz to 25 GHz, and it got 3 dB for lower bands. Hence, the antenna was a very good choice to be applied for UWB applications.

7. Metamaterial (MTM) Structure Antennas

Metamaterials (MTMs) are used widely in communication technology and applications. A low-profile UWB antenna used a right/left- (CRLH-) handed metamaterial structure applied on a composite for wireless communication applications (Figure 14) [81]. The proposed MTM structure comprised three MTM unit cells, a rectangular patch which was cut by two I-shaped slots and a spiral shape inductor that was connected to GND through a via hole. Then, the proposed CRLH MTM used a shunted inductance and a series capacitor.

To make a series capacitance and shunted conductance, a gap and a thin microstrip line were connected to GND through a via. To achieve the capacitance and the inductance, an electromagnetic band gap (EBG) was used. Thereafter, the I-shaped gaps played as the series capacitance (C_l) and spiral gaps played as shunted inductance (L_l). Due to the importance effects of C_l and L_l, they were not avoided. The antenna was mounted on a Rogers RT/duroid 5880 layer with $h = 1.6$ mm, $\varepsilon_r = 2.2$, and loss tanδ 0.0001 with the total dimensions of antenna which were $15 \times 7.87 \times 1.6\,\text{mm}^3$. The antenna attained a wide BW from 3 GHz to 10.6 GHz, a fractional BW of 111%, and a gain of 6.30, 8.56, and 9.41 dBi at frequencies of 5, 8, and 10.5 GHz, respectively. Moreover, the radiation efficiency was 75.40% at 5 GHz, 94% at 8 GHz, and 99.93% at 10.5 GHz.

A planar MTM structure was integrated with a low-profile high-gain microstrip patch antenna for UWB application [82]. The proposed antenna was printed on an FR4 substrate with dielectric constant of 4.4, 1.6 mm height, and total dimensions of $27.6 \times 30.8\,\text{mm}^2$ which had a smaller size in comparison with works in [83, 84]. The patch resonator contained unit cells of π-shaped slots cut from the square-shaped patch and cross-shaped cells which cut from the GND. The back radiations were reduced, and forward radiation patch was improved. Furthermore, to have a better impedance matching, some tapered slots at the end of the microstrip line were used and then fed through the SMA port. Due to the uncovered section of the working BW according to the FCC, the unit cell was cut from the square patch to make it resonated based on the FCC along with improvement in impedance BW. Thus, the proposed antenna had a broad BW from 3-12 GHz and FBW of 119%. Because of the surface current distribution at higher and lower frequencies and the left-handed characteristics, the radiation moved in horizontal direction towards the $x - y$ plane but the vertical direction. The antenna obtained a gain ranging from 1.8 dBi to 5.8 dBi over the UWB range and a 75-95% radiation efficiency over the band. Therefore, the antenna was a promising device for the proposed antenna which can be used for UWB applications.

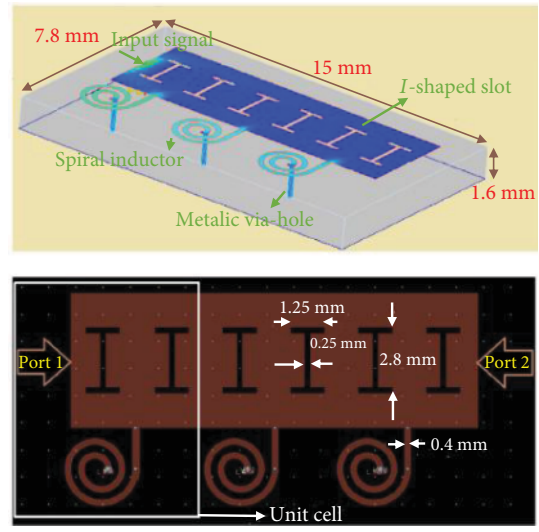

Figure 14: A low-profile UWB antenna used a right/left- (CRLH-) handed metamaterial [81].

An MTM-based low-profile antenna was designed for UWB applications [85]. The MTM cells of the antenna was integrated with the patch and the GND layer. Furthermore, to improve the impedance BW, a slot was cut from the patch near the feeding point. Like the previous research, the proposed antenna had a horizontal radiation after integration with the patch and the GND layer. In addition, the proposed antenna was printed on a FR4 layer with $\varepsilon_r = 4.4$, 0.8 mm height, and overall dimensions of $0.8 \times 27.6\,\text{mm}^2$. To cover the ultra-wideband based on the FCC, a MTM unit cell was etched from the patch near the feed. Thus, it covered all the UWB range based on the FCC and it obtained the working BW 3 GHz up to 14 GHz and the FBW of 129%. It was observed that the antenna attained the maximum radiation efficiency of 94% at 3.5 GHz. Any other way, at higher frequencies due to the loss in substrate, the radiation efficiency was reduced. Furthermore, the antenna got a maximum gain of 7.2 dBi at 13 GHz with a directional pattern. Therefore, the proposed antenna was assumed as a potential device for UWB applications.

A new design of the MTM structure was designed and fed by the CPW technique [86]. An MTM structure was constructed when a SRR and wire were combined properly, and an MTM considers a mixture of two different materials with negative ε and μ. The MTM lens unit cell had the dimensions of $12 \times 10 \times 2\,\text{mm}^3$, and the MTM lens was located parallel to the antenna and at the front of the antenna and at the known distance for better impedance matching. Furthermore, the MTM structure and the SRR were printed on a Rogers substrate. Both gain and directivity of the antenna were increased by 48.77% and 48.12%, respectively, and the radiation efficiency of the antenna improved by 2.65% at higher bands [86].

An MTM structure was designed and fabricated on two planar antennas [87]. The MTM structure consisted of slits

with an *H* shape and inductors with a spiral shape which cut from the radiation patch. Then, a pin connected the spiral to the metallic plane. The method applied in this research reduced the antenna dimensions dramatically compared to the ordinary antenna. Afterward, the antenna was fed by a microstrip line from the left side and then the matched load of 50 Ω was used on the right side of the antenna. The total dimensions of the surface area were $5.4 \times 36.9\,\text{mm}^2$ on a total size of $15 \times 6.9 \times 0.8\,\text{mm}^3$ fabricated on a Rogers Ro4003 layer with $\varepsilon_r = 3.38$ and 0.8 mm height. Other than the compactness, the antenna obtained a wide BW of 1.2-6.7 GHz for VSWR < 2 and FBW of 139%. The antenna had the 6.8 dBi $\text{gain}_{\max}$ and efficiency of 86%. Furthermore, in terms of the time domain consideration, the antenna got 0.25 ns over the BW of 8 GHz. The other T-shaped antenna was printed on a Rogers RO4003 layer with 3.38 permittivity and 0.8 mm height and then fed from both left and right sides. This antenna had the same design procedure. The proposed *T*-shaped antenna attained the impedance BW of 1.1-6.85 GHz for VSWR < 2 with FBW of 144%. The maximum gain and radiation efficiency of the antenna were 7.1 dBi and 91%, respectively. Therefore, both proposed antenna exhibited acceptable and applicable characteristics which suit them for the UWB communication applications such as mobile communications.

8. Printed Elliptical Monopole Antenna

A new design of the UWB monopole elliptical patch was presented for UWB applications [88]. The elliptical patch was printed on a FR4 with $\varepsilon_r = 4.7$ and $h = 1.6$ mm, and the overall size of the antenna was $30 \times 35\,\text{mm}^2$. Furthermore, the GND layer had a rectangular shape which made it unsuitable for UWB antennas (Figure 15). Thus, the antenna height was an effective parameter for impedance BW of the antenna. Besides, GND should be optimized to get a good impedance matching. Initially, the antenna got unacceptable BW for UWB applications based on the FCC, but it improved in later steps. After the improvement, the frequency band was shifted to a higher band. Thus, the maximum gain changed around 2 dBi at 0 degree and 7 dBi at 90 degrees. In addition to that, the antenna was directional except around 8 GHz in which directivity was decreased. Based on the antenna's working BW of 2.9 up to 16 GHz and the measured BW of 3.1-12 GHz, the antenna was able to work for UWB applications.

A UWB BW was presented by an elliptical planar antenna with a single substrate layer [89]. The proposed antenna comprised only one layer of FR4 substrate with 0.8 mm height and $\varepsilon_r = 4.4$, and the rectangular GND layer had a size of $15 \times 20\,\text{mm}^2$. The space between the radiation elements was adjusted for better impedance matching. Furthermore, some slots were cut from the ground to improve the reflection coefficient result of the antenna. In addition to that, the simulated gain over the ultra BW was around 1.39 dBi in boresight. However, the antenna achieved $\text{gain}_{\max}$ and $\text{gain}_{\min}$ (dBi) of 4.16 and 1.39, respectively. The omnidirectional pattern of the antenna was improved by using two orthogonal monopoles. The antenna matched easily and was directly applied for UWB applications.

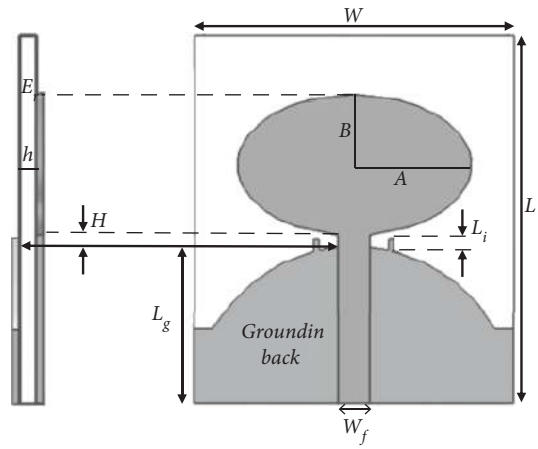

Figure 15: A new design of a UWB monopole elliptical patch was presented for UWB applications [88].

Another UWB dipole antenna with a semi-elliptical shape fed by a microstrip line was designed for UWB communications [90]. This article was an extended version of research presented as follows: both the major and minor axes were interchanged to ease the size reduction process. Moreover, it was found out that most of the energy went through the tapered slot between the radiator and it got the same radiation as the conventional elliptical patch antenna. Therefore, the band notches were removed from the working band by cutting a portion of the radiation patch. To achieve better coupling and impedance matching, the radiation patch was trimmed at its higher edge towards the *z*-direction. After using the tapered shape and considering a gap between them, the antenna was fed by a 50 Ω microstrip line. Moreover, the antenna had a wide impedance BW of 3.05-11.5 GHz for VSWR < 2 while the measured impedance BW was slightly different from the simulated one. Furthermore, the radiation pattern was omnidirectional in the $x - y$ plane. Based on the performances of the antenna, it was suitable for UWB applications.

A new hybrid design of monopole antenna fed by a microstrip antenna was presented in [91]. The proposed antenna comprised an uncompleted GND, the main and parasitic patch in an semi-elliptical shape to obtain a tapered-like structure. The antenna was printed on an FR4 substrate fed by a 50 Ω microstrip line with overall dimensions of 25 mm × 28 mm. In addition, the main patch provided the f_r and the semi-ellipse patch was utilised as a parasitic resonator. The lower edge of BW was reduced when a parasitic plane was used at the back. Furthermore, the parasitic patch acted as a filter since it is related to the band notch. To get other in-band resonances, both main and inverted patches were located separately due to the narrow stub's high impedance. The attenuation level increased with *h*, and the truncated GND acted as an impedance matching circuit. In addition to that, the small alterations in gap width between GND and the main patch affected the reflection coefficient result of the antenna. Moreover, the FBW of the antenna

enhanced from 57% to 120% and the frequency shifted when the parasitic layer was used at the back. Furthermore, the antenna achieved a working BW of 2.7-11 GHz for VSWR < 2. On the other hand, the antenna acted as a conventional monopole printed antenna at the lower and middle parts of the BW, while the pattern of the antenna tilted a bit in the *E*-plane and the cross-polarization enhanced in the *H*-plane. The antenna got a gain range of 0.2-2 dBi for the frequency at 3 GHz to 10 GHz. Besides, both the simulated and measured gain changed in range of 2 to 3.5 dBi. Therefore, the proposed UWB antenna attained an acceptable radiation characteristic to be assumed as device for UWB applications.

An extremely wide BW printed antenna was presented in [92]. To amend the impedance matching of the antenna, the vertical current distribution increased and the horizontal current degraded by using multiple feed lines. The wideband characteristic performances of the antenna were obtained by optimizing the elliptical patch and the GND. In addition, both patch and the GND were mounted on the same side of a substrate with permittivity of 3.48 and 1.524 mm height. The antenna was fed by a modified TSA CPW in between the GND layers, and then the elliptic patch applied three metallic branches: one central and two side branches. Afterward, all the semicircular branches, the tapered CPW, and the elliptical antenna were integrated together. The proposed antenna achieved a wide BW of 24.5 GHz with a ratio of 50 : 1 and an omnidirectional radiation pattern at a lower frequency band in the *H* plane while it got a radiation pattern of a dipole-like radiation pattern in the *E* plane radiation pattern. In addition to that, the radiation efficiency of the antenna was stable at lower frequencies and dropped to 76% at higher frequencies. Therefore, the proposed antenna was capable of integrating with any type of patch-type antenna.

For further studies of the planar UWB antenna, a simple technique of approximation for elliptical patches with a polygon step edge was presented in [93]. For each iteration, it was found out that the polygon was required to have the same dimensions to the elliptical patch. Thus, initially the curved edge elliptical patch was considered as rectangular. Then, it tried to find an optimum point for finding its coordinate to make the patch and the polygon similar in dimensions. To verify the correctness of the proposed method, exemplary numerical simulations were performed. To validate the approximation method, a balun circuit was designed for both circular and second-layer polygon. Thus, a compact rectangular balun was used similar to what was presented. Both antennas were printed on a Taconic RF-35 substrate with the height of 0.762 mm. An impedance BW of the UWB-type antenna achieved 3.1 GHz to 10.6 GHz which showed the same impedance BW as low frequencies but at higher frequencies. Furthermore, they obtained an angular difference from 30 to 60 by maximum of 10 dB. Hence, the results confirmed that a circular or elliptical patch was capable of being approximated by a polygon.

A practical demonstration of a broadband log periodic antenna was presented in [94]. It was known that in log periodic antennas, dimension scaling was periodic and changing with the logarithm of frequencies. The proposed antenna comprised a square patch mounted on an FR4 layer with $\varepsilon_r = 4.4$ and 1.6 mm height, then the antenna was fed by a coaxial cable with 50 ohms. The logarithmic factor was optimized to get VSWR < 2 for the working BW. To improve the results, the substrate's height enhanced. First a rectangular patch was used, but due to the low BW it was changed to an elliptical patch. Thus, a wider BW was obtained. VSWR < 2 for the frequency band of 2.3- 6 GHz. Furthermore, the replacement improved both gain and directivity while it decreased the side and back lobes. Finally, it was proved that by choosing a proper material, the proposed replacement achieved a wider BW.

Due to the importance of the wireless body area network (WBAN) in UWB applications, a compact and miniaturized elliptical patch fed by the CPW technique was presented in [95]. Both patch and the feeding line were printed on the same side of the board with $h = 0.695$ mm, the gap between the GND and patch was optimized. The antenna had dimensions of $15 \times 10\,\text{mm}^2$ for patch and total dimensions of $35 \times 45 \times 2\,\text{mm}^3$. Furthermore, the antenna was used for a human body tissue with the dimensions of 45 mm × 55 mm × 26 mm. It used three layers of skin, fat, and muscle, and their electronic properties were presented. The antenna achieved a wide BW of around 12 GHz in the range of 2.39-14.43 GHz with VSWR < 2. The antenna's power radiated mostly in the left and right hand towards 107 degrees, and it got an omnidirectional radiation pattern. In addition to that, the antenna presented directivity, gain, and radiation efficiency of 5.218 dBi, 5.132 dB, and 97%, respectively. Due to the wide BW, a very small number of signals reflected to the source. To investigate the effect of the human body, a three-layered phantom was developed. After integration of the antenna with the human body, the antenna got a directive pattern especially at higher frequencies. Thus, the antenna was used for wireless body area network (WBAN) applications.

9. Flexible Wearable Antennas

A low-profile, compact-size, planar flexible antenna was designed on a natural rubber substrate for UWB applications. It was the first time that a rubber with natural properties was used as a substrate for UWB antennas and applications. This UWB antenna was simulated for WBAN as a revolution of the sensor network (Figure 16) [96].

The antenna fed by the CPW technique as both resonator and GND were on the same layer; therefore, feeding's characteristics gave performances such as wider BW, improved matching, and ease of integration with active devices. The proposed antenna was built on FR4 with 1 mm height, $\varepsilon_r = 4.4$, and 0.02 tanδ with an overall size of $42 \times 46\,\text{mm}^2$ without metallization. The design procedure started by choosing the lower and higher edges of the antenna with a shape of a rhomboid. Moreover, the rubber substrate had 1.2 mm thickness with $\varepsilon_r = 9.3897$ and tanδ of 0.015 and dimensions of $42 \times 34\,\text{mm}^2$, with no metallic layer behind the antenna. The antenna achieved a wide BW of 3.1 GHz to 10.6 GHz as lower and higher ends of the UWB band. Moreover, the

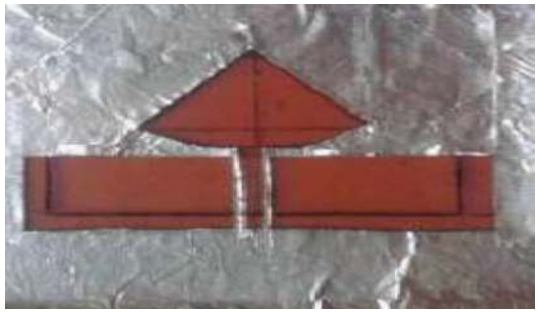

Figure 16: A low-profile, compact-sized, planar flexible antenna designed on a natural rubber substrate [96].

antenna obtained VSWR < 2 for all the working BW and indicated a good impedance matching. The antenna achieved a maximum gain of 1.7 dB and 8 dB on the FR4 substrate and rubber substrate, respectively. An omnidirectional radiation pattern was obtained for both the antenna and the 90% radiation efficiency. Being more precise, the antenna with the FR4 substrate had 97% efficiency and 93% of the rubber substrate. Therefore, the antenna met the UWB application requirements to be applied for WBAN.

Another UWB wearable antenna for on-body applications was investigated for indoor environment. The proposed antenna was designed for the range of 3-10 GHz comprising a compact, low-profile TSA antenna [97]. The total dimensions of the antenna were 27 mm × 16 mm with a gain range of −2 to 2 dBi and radiation efficiency of around 80% and 63% in free space and on the body, respectively. In the measurement procedure, the antenna was located on the shoulder, elbow, and wrist for the limbs. These places were chosen based on the ease of use and daily activity. In addition, the mobile stations were put in different distances for each wearable antenna. After optimizing the distances, it was noticed that the best result was obtained when the distances were from 0.5 cm to 1.5 cm. Because of the wide BW and high radiation characteristics, the proposed UWB antenna was a good choice for WBAN application.

A high-fidelity UWB antenna was designed for on-body applications using textile substrate. The antenna had an octagonal patch and was fed by the CPW technique [98]. Furthermore, to exceed the BW, the octagonal patch used the bevel method [99]. Thus, the antenna got the initial maximum dimensions of $40.23 \times 45.18\,\text{mm}^2$ after optimizations. Besides, the antenna had an operating BW of 2 to 12 GHz with an initial bidirectional radiation pattern which considered as a drawback for this application. Hence, to evade the body effects on the antenna performances, a full-layered GND was applied to act as a reflector. Then, a parasitic patch was used to meet the compact antenna requirements along with BW increase. Therefore, the final design of the antenna was a multistacked antenna fed by CPW and a full-layer reflector. As aforementioned, the antenna used two substrate layers and three metallic layers and final dimensions of $80 \times 61 \times 4.51\,\text{mm}^3$. Since the measured radiation pattern showed a radiation away from the body, the low level of coupling was obtained. The antenna achieved the 7.2 dBi gain_{max} at 9 GHz. In addition to that, the antenna had a gain lower than 5 dBi for a frequency band less than 5 GHz. Furthermore, the antenna attained the maximum and minimum SAR values of 1.21 W/kg at 3 GHz and 0.52 W/kg at 7 GHz, respectively. The antenna had the working BW of 7.82 GHz suitable for UWB and WBAN applications.

Another UWB-flexible antenna was designed for a wearable application working band of 3.7–10.3 GHz which was tolerated for the human body [100]. Two arc-shaped patch antennas were printed on a polyglycerol monostearate (PGMS) layer with $\varepsilon_r = 2.7$ and variable $\tan\delta$ from 0.02 to 0.07 designed for UWB applications. Furthermore, the antenna reused conductors like nickel– copper–silver-coated nylon ripstop with a thickness of 0.13 mm because of high conductivity as a patch layer and another layer of 0.08 mm used for the GND layer [101]. The results showed an impedance matching in band of 3.7–10.3 GHz for stable VSWR < 2. The full layer of GND helped to have a good radiation efficiency and avoid the effect of the body on the antenna. In addition to that, the proposed antenna illustrated SFF of 0.88, 0.77, and 0.72 in free space. After measurement on the body at 6 GHz, a wide BW, maximum gain of 4.53 dBi, and total efficiency of 27% achieved. A SAR factor of the antenna was less than 2 W/kg with input power of 0.5 W. Therefore, the antenna's time domain performance illustrated that the antenna was suitable for UWB applications.

A new printed flexible wearable antenna was designed for UWB applications [102]. Due to the circular and elliptical patch performances towards the conventional patch, an elliptical shape was used as an initial shape of design [103]. Hence, the antenna used an elliptical patch fed by CPW techniques with a material of PANI/MWCNTs with 110 μm height for the GND layer and kapton substrate with permittivity of 3.48 and 0.002 loss tangent. After simulation, the antenna was put on a cloth for further investigations and any movements were checked. Then the crumpling and uncrumpling impacts were studied well. The antenna showed a wide BW with a good reflection coefficient result near 30 dB when it was bended towards the y-axis. The antenna bending created two in-band resonances at 2.2 and 5.3 GHz. The designed in-band frequencies for both crumpled and un-crumpled were 1.9, 2.45, 5.4, and 5.8 GHz. Besides, the antenna presented omni- and bidirectional patterns in E and H planes, respectively. The crumpled antenna had a cross-polarization similar to a dipole antenna with minimum gain at 0 and 180 degrees and maximum at ±90 degrees. Therefore, the antenna showed promising results for wireless communications especially when it integrated on clothes.

An antenna with textile material as substrate and semi-elliptical GND shaped antenna was printed for UWB communications [104]. The antenna had high R_r next to 50 Ω and low R_s close to 0. The antenna was designed and fabricated on nonwoven polyester with dimensions of $80.0 \times 70.0\,\text{mm}^2$, and it comprised a resonator with triangular shape fed by a microstrip line. A square-shaped cut from the GND layer was used to amend the BW. After optimization of

antenna dimensions, it was noticed that it was capable of working as a tuneable multiband antenna. Thus, the antenna showed impedance BW of 3.4 to 11.6 GHz, and more resonances at 1.4 to 1.6 GHz, 1.85 to 2 4 GHz, and radiation efficiency of 60%. Furthermore, the antenna had an omnidirection in the *E*-plane with a low level of cross-polarization. Based on the presented result, the proposed antenna was applicable for GPS, PCS-1900, IMT-2000/UMTS, and WiFi.

A textile wearable UWB antenna was presented for WBAN applications [105]. Shieldit Super as a conductor and a felt substrate with thickness of 0.17 mm were used. The felt substrate had height of 3 mm, 1.45 permittivity, and loss tangent of 0.044. Furthermore, the antenna used four radiators, A and B as patches, and a parasitic patch which operated from 3.4 to 10.2 GHz. In this design, the capacitive coupling had most effects on the BW of the antenna [106]. The antenna obtained the measured BW of 3.6-10.3 GHz and a maximum gain of 7.75 dB at 10 GHz. Then to measure on the body, a sample with dimensions of $131 \times 121 \times 44\,\text{mm}^3$ and relative permittivity of 50.8 was used. In each step of the measurement, the location of the antenna on the body and the gap between the body and antenna were optimized to get the best result. The full layer of GND improved the SAR layer and played as a reflector, and after placing ATA-FGP on the body, the antenna's radiation efficiency reduced by 1.2%. Due to using a quite large ground layer, the coupling and consequently the SAR level decreased.

A compact and low-profile flexible wearable antenna was designed to integrate with electronic components [107]. Due to the need of an omnidirectional pattern and high-performance radiation characteristics of the antenna for most of the applications, a UWB antenna was designed in this paper. The proposed antenna was printed on a DuPont Kapton polyimide substrate with thickness of 50.8 μm, permittivity of 3.4, and overall dimensions of 30 mm × 33 mm, and then the antenna was fed by the CPW technique to have a low cost since both the radiator and the GND were on the same layer. Furthermore, the proposed antenna achieved a simulated operating BW from 2.3 GHz to 15.2 GHz and 3.1–12.9 GHz measured one. Thus, the proposed antenna covered the required BW of UWB standard. Besides, the radiation pattern of the antenna maintained its omnidirectional pattern for most of the band. Therefore, due to the antenna's advantages like flexibility, mechanical robustness, small size, and acceptable radiation pattern, it worked for UWB applications.

A band notch TSA wearable UWB antenna was designed in [108]. The proposed antenna used a liquid crystal polymer (LCP) layer with $\varepsilon_r = 2.9$ and 0.05 mm and 0.018 mm height for the substrate and the conductor, respectively. The substrate had significant characteristics such as ultra-thin, flexible, light, and cheap with 0.004 low water absorption factor, 0.002 dissipation factor, and low permeability. Thus, the antenna was applicable for any environment with physical robustness. The tapered slot had a significant effect in BW widening along with two ellipses which improved the matching [109]. The proposed antenna had total dimensions $26 \times 16 \times 0.068\,\text{mm}^3$. However, to avoid the interference at a higher WLAN frequency band (5.15–5.35 GHz), it was cut out of the BW by making an H-shaped slot close to the feeding. Furthermore, the antenna's performances were investigated in different bending angles of 15°, 30°, 45°, and 60°. The proposed antenna covered all UWB frequency ranges except 5.25 GHz. Both simulation and measurement results were in good agreement, and the antenna showed improvement in degraded factors. In addition to that, the proposed antenna had an omni pattern and dipole-like pattern for *H* and *E* planes with a stability over the BW. Although the antenna showed reduction in radiation efficiency after integration with the body, it achieved a reasonable gain of 2-3 dBi and maximum efficiency of 99% at 9 GHz. Therefore, the proposed antenna illustrated promising results in free space and on body integration even under harsh conditions of bending and it proved that it was a good choice for indoor UWB communication applications.

Although many other review papers and books exist that presented the importance of UWB antennas and their applications, the presented paper here tried to offer a good guidance for the readers with concise and detailed information [1, 109–115].

10. Dielectric Resonator Antenna (DRA)

Dielectric resonator antennas (DRAs) have been assumed as a promising variant of conventional antennas since 1983 [9]. Many DRAs exist for various applications like communications [116, 117]. DRA was used for many purposes such as making and improving the band notch to ignore the interference in a frequency band using high-permittivity slabs [118]. Besides, DRAs showed good performances in creating compact-sized antennas [119].

In the case of making band notch applying DRA, many works were performed with different structures and shapes. Table 2 shows some recent DRAs along with their performances.

11. Conclusion

A comprehensive review concerning broadband, multiband, and UWB antennas for wireless communication systems was performed in this paper. Geometries, materials, design solutions, and numerical tools adopted for the analysis and design were investigated. Several types and shapes of antennas useful for communication applications were presented. The electromagnetic performances, the dimensions, and the materials, as well as the design solutions useful to improve the antenna bandwidth of monopole (2D and 3D profile), printed planar antennas, metamaterials, tapered and wide slot antennas, and elliptical patch printed and wearable antennas were presented here. The investigation was carried out in this review paper; the following are general considerations concerning the presented antennas' challenges (Table 3).

When monopole antennas are located on a metallic plate as a GND, this GND layer emits energy throughout the spatial region; thus, while designing the antenna the shape and

Table 2: DRAs' comparisons.

Antenna	Dimensions	BW	References
Bi-cone DRA	$7.58\,cm^3$	2.8-7.38 GHz	[120]
U-shaped DRA	$30 \times 42\,mm^2$	2.65-10.9 GHz	[121]
MIMO DRA	$29 \times 29 \times 5\,mm^3$	4.98-6.08 GHz	[122]
Balanced dual-segment cylindrical DRA	$23 \times 23\,mm^2$	6.4- 11.736 GHz	[123]
Compact UWB DRA	$12 \times 30 \times 6\,mm^3$	3.22-4.06 and 4.84-5.96 GHz	[124]
UWB DRA cognitive radio	$150 \times 150\,mm^2$	2.4–12 and 2.3-4.5 GHz	[125]

the geometry should be considered. In addition, it was shown that when the antenna is excited from more than one port, the antenna's performances such as operating BW, polarization, and signal integrity especially for the UWB antenna were improved.

In addition to that, the GND plane restricted the interference with the sensitive electronic circuitry existing in the antenna's back region and the inherent 3D geometry limits their use to applications concerning base stations as well as automotive or avionic systems for high-speed vehicles.

Many antennas were designed to have a wide BW by applying different shapes and techniques such as using meta-surfaces and blind-filled cylinder holes to improve the radiation pattern along with the increase in BW. Moreover, it showed that cutting the Vivaldi antenna and creating a slot between three parts of its patch could improve the BW and change the antenna with a narrow band to a wide band. Besides, it was able to increase the radiation characteristics of the antenna. In addition to that, techniques like using vias to shorting walls, split ring resonators to improve the BW and CP performance, periodic structures like EBG and DBG, and SIW as balun were used to improve the wideband antennas' performances.

Wide-slot antennas were used widely in applications that need a wide BW. To obtain a wide BW and acceptable VSWR, an absorber was used with the GND layer. Furthermore, a combination of elliptical and circular slots from the GND layer and triangular slots from the patch was used to have a better tool for impedance matching and BW. Another improvement in BW and antenna performance was obtained using TSIR and PSLR. Some methods were performed to reduce the antenna's dimensions and create a stack antenna. For instance, a TTDMESS-based CP reflect array was used to decrease the antenna's dimensions. In designing a procedure of stack antennas, optimizing the layer's thickness affects the Q-factor and the BW.

The TSA antennas were applied for UWB communication applications since a long time ago. The slot is usually cut based on the low and high frequency of the antenna. By optimizing the exponential slot dimensions, the coupling can be taken care of. Moreover, cutting the slot from the patch shows improvement in BW in the UWB antenna. In addition to that, a Chebyshev mathematical approach is designed to model the slot and smoothen the design steps.

Printed monopoles exhibit a low profile that allows using both fixed (base stations, automotive systems, etc.) and mobile terminals (smartphones, tablets, glasses, laptops, wearable computers, etc.), as well as a simple integration with the RF circuits. The use of dielectric materials implies the presence of surface waves; therefore, the use of thin dielectric materials having low dielectric permittivity is strongly recommended. Furthermore, the dielectric materials used as substrate should be chosen carefully to avoid the unwanted coupling between the antenna and the medium (like body). When designing the UWB antennas was important, the interference among the frequency bands such as WLAN and WiMax became critical. Hence, many techniques could be applied to filtering these bands like making notches on the patch or the GND layer. But it should be noticed that these filters are responsible for an alteration of the group delay, which can result in a significant distortion of the radiated signal with the appearance of a pronounced ringing. Therefore, the designing procedure should be done carefully. These problems are more tangible when the MTM structure is utilised due to the achieved electromagnetic performances. To overcome these drawbacks, additional research activities should be performed to find new metamaterial geometries suitable to guarantee stable group delay and limited ringing effects.

When an elliptical shape is chosen for patches, the antenna can be a simple antenna working as an UWB antenna without adding any complexity to the antenna like loading the antenna. The elliptical patch UWB antenna can be optimized in the minor axis of the patch to get a wider WB. The space between the ground at the back and the junction of the transmission line and the patch is another parameter which is important in obtaining the wide BW.

Wearable antennas require additional design parameters that should be considered. For instance, when they are integrated with the human body, the user's body should be shielded as much as possible from the electromagnetic field generated by the antenna. This interaction increases energy deposition towards the user's body which causes degraded efficiency and changing the radiation patterns. To solve this problem, a full GND layer is useful. Moreover, for the wearable antennas, development of dedicated transitions, connectors, and flexible feeding lines to be easily integrated with the e-textiles would be desirable.

Table 3: A brief comparison of applied UWB antennas for communication applications.

Antennas	Advantages	Disadvantages	Prototypes
Stacked patch antenna [60]	Good radiation characteristic Allowing a suitable time-domain characteristic	Directive Complicated structure	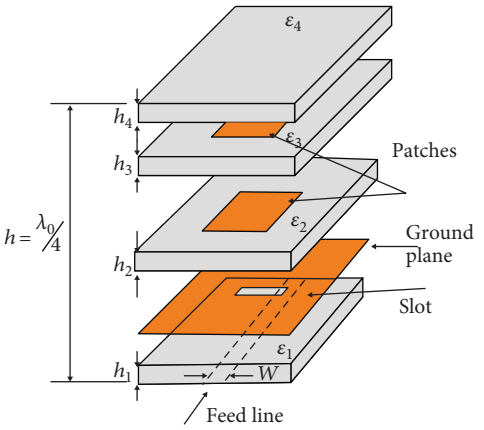
Vivaldi antenna [67]	Can yield a large bandwidth	Complicated structure	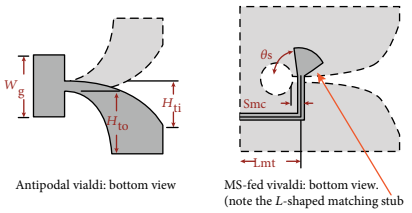
Wide-slot antenna [48]	Can obtain a wide impedance bandwidth if the distance between the radiating arms and ground place is selected properly	Large size at the frequency band of interest	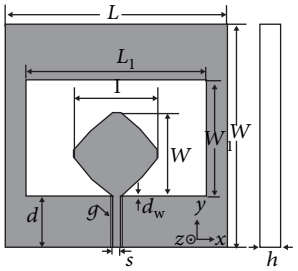
Taper slot antenna [67]	(i) High gain at high frequency (ii) Symmetric beamwidths	High cross-polarization level	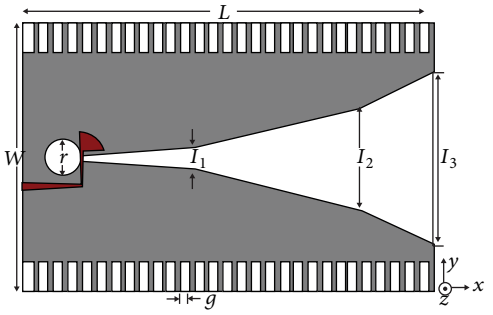
Printed elliptical monopole antenna [88]	(i) Wide bandwidth can be achieved (ii) Simple structure (iii) Size suitable array design (iv) Height—few mm (v) Easily mounted on ordinary plastic casing (vi) Broadside radiator with an omnidirectional radiation pattern (vii) 3D radiation pattern		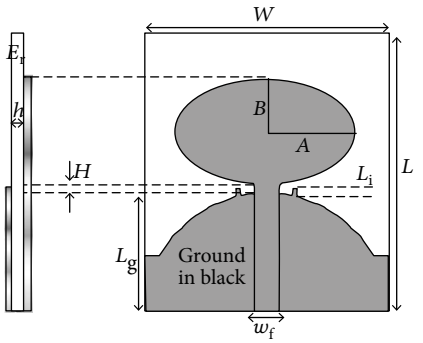

Conflicts of Interest

The authors declare that there is no conflict of interest regarding the publication of this paper.

Acknowledgments

We thank Universiti Teknologi Petronas' YUTP grant for supporting.

References

[1] R. Cicchetti, E. Miozzi, and O. Testa, "Wideband and UWB antennas for wireless applications: a comprehensive review," *International Journal of Antennas and Propagation*, vol. 2017, Article ID 2390808, 45 pages, 2017.

[2] J. D. Kraus and R. J. Marhefka, *Antennas for All Applications*, McGraw-Hill Higher Education, 3rd edition, 2002.

[3] R. Garg, P. Bhartia, I. J. Bahl, and A. Ittipiboon, *Microstrip Antenna Design Handbook*, Artech House, 2001.

[4] R. Cicchetti, A. Faraone, D. Caratelli, and M. Simeoni, "Wideband, multiband, tunable, and smart antenna systems for mobile and UWB wireless applications 2014," *International Journal of Antennas and Propagation*, vol. 2015, Article ID 536031, 3 pages, 2015.

[5] G. M. Galvan-Tejada, M. A. Peyrot-Solis, and H. J. Aguilar, *Ultra Wideband Antennas: Design, Methodologies, and Performance*, Taylor & Francis Group, 2017.

[6] T. A. Denidni and G. Augustin, *Ultrawideband Antennas for Microwave Imaging Systems*, Artech House, Norwood, MA, USA, 2014.

[7] D. Valderas, J. I. Sancho, D. Puente, C. Ling, and X. Chen, *Ultrawideband Antennas: Design and Applications*, Imperial College Press, London, UK, 2011.

[8] M. Ghavami, L. B. Michael, and R. Kohno, *Ultra Wideband Signals and Systems in Communication Engineering*, John Wiley & Sons, Ltd, Chichester, UK, 2007.

[9] S. K. K. Dash, T. Khan, and Y. M. M. Antar, "A state-of-art review on performance improvement of dielectric resonator antennas," *International Journal of RF and Microwave Computer-Aided Engineering*, vol. 28, no. 6, article e21270, 2018.

[10] J. Howell, "Microstrip Antennas," in *1972 Antennas and Propagation Society International Symposium*, pp. 177–180, Williamsburg, VA, USA, 1972.

[11] K. C. Gupta and A. Benalla, "Microstrip antenna design," in *Technology & Engineering*, Artech House, 1988.

[12] P. Wang and Z. Shen, "End-fire surface wave antenna with metasurface coating," *IEEE Access*, vol. 6, pp. 23778–23785, 2018.

[13] Y. Zhao, Z. Shen, and W. Wu, "Wideband and low-profile H-plane ridged SIW horn antenna mounted on a large conducting plane," *IEEE Transactions on Antennas and Propagation*, vol. 62, no. 11, pp. 5895–5900, 2014.

[14] A. R. Mallahzadeh and S. Esfandiarpour, "Wideband H-plane horn antenna based on ridge substrate integrated waveguide (RSIW)," *IEEE Antennas and Wireless Propagation Letters*, vol. 11, pp. 85–88, 2012.

[15] Y. Dong, J. Choi, and T. Itoh, "Vivaldi antenna with pattern diversity for 0.7 to 2.7 GHz cellular band applications," *IEEE Antennas and Wireless Propagation Letters*, vol. 17, no. 2, pp. 247–250, 2018.

[16] R. A. Marino, "Broadband fixed-radius slot antenna arrangement," US Patent 6043785.

[17] Y. Yang, Y. Wang, and A. E. Fathy, "Design of compact vivaldi antenna arrays for UWB see through wall applications," *Progress In Electromagnetics Research*, vol. 82, pp. 401–418, 2008.

[18] N. W. Liu, L. Zhu, and W. W. Choi, "A low-profile wide-bandwidth planar inverted-F antenna under dual resonances: principle and design approach," *IEEE Transactions on Antennas and Propagation*, vol. 65, no. 10, pp. 5019–5025, 2017.

[19] Y. Lo, D. Solomon, and W. Richards, "Theory and experiment on microstrip antennas," *IEEE Transactions on Antennas and Propagation*, vol. 27, no. 2, pp. 137–145, 1979.

[20] S. Yan, V. Volskiy, and G. A. E. Vandenbosch, "Compact dual-band textile PIFA for 433-MHz/2.4-GHz ISM bands," *IEEE Antennas and Wireless Propagation Letters*, vol. 16, pp. 2436–2439, 2017.

[21] G. Varshney, V. S. Pandey, R. S. Yaduvanshi, and L. Kumar, "Wide band circularly polarized dielectric resonator antenna with stair-shaped slot excitation," *IEEE Transactions on Antennas and Propagation*, vol. 65, no. 3, pp. 1380–1383, 2017.

[22] Y. Zhang, Z. Xue, and W. Hong, "Planar substrate-integrated endfire antenna with wide beamwidth for Q-band applications," *IEEE Antennas and Wireless Propagation Letters*, vol. 16, pp. 1990–1993, 2017.

[23] T. Zhang, Y. Zhang, L. Cao, W. Hong, and K. Wu, "Single-layer wideband circularly polarized patch antennas for Q-band applications," *IEEE Transactions on Antennas and Propagation*, vol. 63, no. 1, pp. 409–414, 2015.

[24] R. A. Alhalabi and G. M. Rebeiz, "High-efficiency angled-dipole antennas for millimeter-wave phased array applications," *IEEE Transactions on Antennas and Propagation*, vol. 56, no. 10, pp. 3136–3142, 2008.

[25] P. Wang and Z. Cai, "Planar printed loop antenna with less no-ground space for hepta-band wireless wide area network/-long-term evolution mobile handset," *Electronics Letters*, vol. 52, no. 15, pp. 1284–1286, 2016.

[26] C. Zhao and C.-F. Wang, "Characteristic mode design of wide band circularly polarized patch antenna consisting of H-shaped unit cells," *IEEE Access*, vol. 6, pp. 25292–25299, 2018.

[27] C. H. See, R. A. Abd-Alhameed, D. Zhou, T. H. Lee, and P. S. Excell, "A crescent-shaped multiband planar monopole antenna for mobile wireless applications," *IEEE Antennas and Wireless Propagation Letters*, vol. 9, pp. 152–155, 2010.

[28] S. H. Chang and W. J. Liao, "A broadband LTE/WWAN antenna design for tablet PC," *IEEE Transactions on Antennas and Propagation*, vol. 60, no. 9, pp. 4354–4359, 2012.

[29] M. Crepaldi, D. Dapra, A. Bonanno, I. Aulika, D. Demarchi, and P. Civera, "A very low-complexity 0.3–4.4 GHz 0.004 mm^2 all-digital ultra-wide-band pulsed transmitter for energy detection receivers," *IEEE Transactions on Circuits and Systems I: Regular Papers*, vol. 59, no. 10, pp. 2443–2455, 2012.

[30] H. Zhu and J. Mao, "Miniaturized tapered EBG structure with wide stopband and flat passband," *IEEE Antennas and Wireless Propagation Letters*, vol. 11, no. 3, pp. 314–317, 2012.

[31] A. L. Borja, A. Belenguer, J. Cascon, H. Esteban, and V. E. Boria, "Wideband passband transmission line based on metamaterial-inspired CPW balanced cells," *IEEE Antennas*

and Wireless Propagation Letters, vol. 10, pp. 1421–1424, 2011.

[32] Y. Xu, C. Nerguizian, and R. G. Bosisio, "Wideband planar Goubau line integrated circuit components at millimetre waves," *IET Microwaves, Antennas & Propagation*, vol. 5, no. 8, p. 882, 2011.

[33] B. Rahmati and H. R. Hassani, "Multi-notch slot loaded wide band planar plate monopole antenna," *IET Microwaves, Antennas & Propagation*, vol. 4, no. 12, p. 2160, 2010.

[34] M. S. Lin, Y. H. Huang, and C. I. G. Hsu, "Design a dual-band high-impedance surface structure for electromagnetic protection in WLAN applications," in *2014 International Symposium on Electromagnetic Compatibility*, pp. 525–528, Tokyo, Japan, 2014.

[35] M.-S. Lin, C.-H. Huang, and C. I. G. Hsu, "Performance study of electromagnetic protective sheets for wireless communication systems," in *2012 Asia-Pacific Symposium on Electromagnetic Compatibility*, pp. 725–728, Singapore, 2012.

[36] R. T. Remski, "Analysis of photonic bandgap surfaces using Ansoft HFSS," *Microwave Journal*, vol. 53, pp. 190–198, 2000.

[37] D. K. Nandanwar and S. S. Pawar, "Analysis of elliptical planar metal plate monopole antenna with different feeding strip length for UWB application," *International Journal of Advanced Technology in Engineering and Science*, vol. 2, pp. 532–536, 2014.

[38] L. Y. Chen, Z. R. Li, H. Zhang, X. Q. Zhang, X. F. Wu, and Y. Yang, "A planar metal-plate monopole antenna for indoor DTV applications," *Journal of Electromagnetic Waves and Applications*, vol. 26, no. 11-12, pp. 1538–1544, 2012.

[39] W.-S. Lee, W. G. Lim, and J.-W. Yu, "Multiple band-notched planar monopole antenna for multiband wireless systems," *IEEE Microwave and Wireless Components Letters*, vol. 15, no. 9, pp. 576–578, 2005.

[40] M. J. Ammann and Z. N. Chen, "Wideband monopole antennas for multi-band wireless systems," *IEEE Antennas and Propagation Magazine*, vol. 45, no. 2, pp. 146–150, 2003.

[41] K.-L. Wong, C.-H. Wu, and S.-W. Su, "Ultrawide-band square planar metal-plate monopole antenna with a trident-shaped feeding strip," *IEEE Transactions on Antennas and Propagation*, vol. 53, no. 4, pp. 1262–1269, 2005.

[42] Y. T. Liu and C. W. Su, "Wideband omnidirectional operation monopole antenna," *Progress In Electromagnetics Research Letters*, vol. 1, pp. 255–261, 2008.

[43] J. D. Kraus, *Antennas*, McGraw-Hill, 2nd edition, 1988.

[44] S.-W. Su, K.-L. Wong, and C.-L. Tang, "Ultra-wideband square planar monopole antenna for IEEE 802.16a operation in the 2–11-GHz band," *Microwave and Optical Technology Letters*, vol. 42, no. 6, pp. 463–466, 2004.

[45] J. Martínez-Fernández, J. M. Gil, and J. Zapata, "Profile optimisation in planar ultra-wideband monopole antennas for minimum return losses," *IET Microwaves, Antennas & Propagation*, vol. 4, no. 7, pp. 881–892, 2010.

[46] J. Rubio, J. Arroyo, and J. Zapata, "SFELP—an efficient methodology for microwave circuit analysis," *IEEE Transactions on Microwave Theory and Techniques*, vol. 49, no. 3, pp. 509–516, 2001.

[47] K. Sneha and N. N. Sastry, "Wide band printed ring circular slot radiator," in *Proceedings of the World Congress on Engineering (WCE 2017)*, pp. 7–10, London, UK, 2017.

[48] A. Wu and B. Guan, "Printed slot antennas for various wideband applications using shape blending," *International Journal of RF and Microwave Computer-Aided Engineering*, vol. 26, no. 1, pp. 3–12, 2016.

[49] Y.-W. Zhong, G. M. Yang, and L. R. Zheng, "Planar circular patch with elliptical slot antenna for ultrawideband communication applications," *Microwave and Optical Technology Letters*, vol. 57, no. 2, pp. 325–328, 2015.

[50] Y. Li, W. Li, and Q. Ye, "A CPW-fed circular wide-slot UWB antenna with wide tunable and flexible reconfigurable dual notch bands," *The Scientific World Journal*, vol. 2013, Article ID 402914, 10 pages, 2013.

[51] T. Aboufoul, A. Alomainy, and C. Parini, "Reconfigured and notched tapered slot UWB antenna for cognitive radio applications," *International Journal of Antennas and Propagation*, vol. 2012, Article ID 160219, 8 pages, 2012.

[52] Y. Li, W. Li, and R. Mittra, "A cognitive radio antenna integrated with narrow/ultra-wideband antenna and switches," *IEICE Electronics Express*, vol. 9, no. 15, pp. 1273–1283, 2012.

[53] Y. Li, W. Li, and Q. Ye, "Miniaturization of asymmetric coplanar strip-fed staircase ultrawideband antenna with reconfigurable notch band," *Microwave and Optical Technology Letters*, vol. 55, no. 7, pp. 1467–1470, 2013.

[54] B. Li, J. Hong, and B. Wang, "Switched band-notched UWB/-dual-band WLAN slot antenna with inverted S-shaped slots," *IEEE Antennas and Wireless Propagation Letters*, vol. 11, pp. 572–575, 2012.

[55] N. Choudhary, A. Tiwari, K. G. Jangid et al., "Design of CPW fed printed slot antenna with circular polarization for UWB application," in *AIP Conference Proceedings*, pp. 1–5, Rajasthan, India, 2016.

[56] M. B. Kakhki and P. Rezaei, "Reconfigurable microstrip slot antenna with DGS for UWB applications," *International Journal of Microwave and Wireless Technologies*, vol. 9, no. 7, pp. 1517–1522, 2017.

[57] Q. Wu, R. Jin, J. Geng, and M. Ding, "Printed omnidirectional UWB monopole antenna with very compact size," *IEEE Transactions on Antennas and Propagation*, vol. 56, no. 3, pp. 896–899, 2008.

[58] R. Singha, D. Vakula, and N. V. S. N. Sarma, "Compact concentric ring shaped antenna for ultra wide band applications," *IOP Conference Series: Materials Science and Engineering*, vol. 67, 2014.

[59] C.-Y. Liu, T. Jiang, and Y.-S. Li, "A compact wide slot antenna with dual band-notch characteristic for ultra wideband applications," *Journal of Microwaves, Optoelectronics and Electromagnetic Applications*, vol. 10, no. 1, pp. 55–64, 2011.

[60] S. M. A. M. H. Abadi and N. Behdad, "Broadband true-time-delay circularly polarized reflectarray with linearly polarized feed," *IEEE Transactions on Antennas and Propagation*, vol. 64, no. 11, pp. 4891–4896, 2016.

[61] M. N. Shakib, M. Moghavvemi, and W. N. L. Mahadi, "A low-profile patch antenna for ultrawideband application," *IEEE Antennas and Wireless Propagation Letters*, vol. 14, pp. 1790–1793, 2015.

[62] H. Malekpoor and S. Jam, "Miniaturised asymmetric E-shaped microstrip patch antenna with folded-patch feed," *IET Microwaves, Antennas & Propagation*, vol. 7, no. 2, pp. 85–91, 2013.

[63] M. N. Shakib, M. T. Islam, and N. Misran, "Stacked patch antenna with folded patch feed for ultra-wideband

application," *IET Microwaves, Antennas & Propagation*, vol. 4, no. 10, pp. 1456–1461, 2010.

[64] D. Gibbins, M. Klemm, I. J. Craddock, J. A. Leendertz, A. Preece, and R. Benjamin, "A comparison of a wide-slot and a stacked patch antenna for the purpose of breast cancer detection," *IEEE Transactions on Antennas and Propagation*, vol. 58, no. 3, pp. 665–674, 2010.

[65] R. Nilavalan, I. J. Craddock, A. Preece, J. Leendertz, and R. Benjamin, "Wideband microstrip patch antenna design for breast cancer tumour detection," *IET Microwaves, Antennas & Propagation*, vol. 1, no. 2, p. 277, 2007.

[66] M. A. Matin, B. S. Sharif, and C. C. Tsimenidis, "Dual layer stacked rectangular microstrip patch antenna for ultra wideband applications," *IET Microwaves, Antennas & Propagation*, vol. 1, no. 6, p. 1192, 2007.

[67] K. S. Naik, D. Madhusudan, and S. Aruna, "Slot tapered Vivaldi antenna with corrugated edges," *Advanced Science and Technology Letters*, vol. 147, pp. 142–149, 2017.

[68] Y. Zhang and A. K. Brown, "Bunny ear combline antennas for compact wide-band dual-polarized aperture array," *IEEE Transactions on Antennas and Propagation*, vol. 59, no. 8, pp. 3071–3075, 2011.

[69] S. W. Kim and D. Y. Choi, "Implementation of rectangular slit-inserted ultra-wideband tapered slot antenna," *SpringerPlus*, vol. 5, no. 1, p. 1387, 2016.

[70] S. W. Kim, G. S. Kim, S. K. Noh, and D. Y. Choi, "Design and implementation of an IR-ultra wide band tapered slot antenna with a rectangular slot structure," in *International Conference on Green and Human Information Technology*, pp. 321–324, Da Nang, Vietnam, 2015.

[71] K. Ebnabbasi, S. Sczyslo, and M. Mohebbi, "UWB performance of coplanar tapered slot antennas," *IEEE Antennas and Wireless Propagation Letters*, vol. 12, pp. 749–752, 2013.

[72] W. Sörgel and W. Wiesbeck, "Influence of the antennas on the ultrawideband transmission," *EURASIP Journal on Advances in Signal Processing*, vol. 2005, no. 3, Article ID 843268, 2005.

[73] J. Wu, Z. Zhao, Z. Nie, and Q.-H. Liu, "A printed UWB Vivaldi antenna using stepped connection structure between slotline and tapered patches," *IEEE Antennas and Wireless Propagation Letters*, vol. 13, pp. 698–701, 2014.

[74] A. Z. Hood, T. Karacolak, and E. Topsakal, "A small antipodal Vivaldi antenna for ultrawide-band applications," *IEEE Antennas and Wireless Propagation Letters*, vol. 7, pp. 656–660, 2008.

[75] Z. H. Tu, W. A. Li, and Q. X. Chu, "Single-layer differential CPW-fed notch-band tapered-slot UWB antenna," *IEEE Antennas and Wireless Propagation Letters*, vol. 13, pp. 1296–1299, 2014.

[76] K. Kikuta and A. Hirose, "Compact folded-fin tapered slot antenna for UWB applications," *IEEE Antennas and Wireless Propagation Letters*, vol. 14, pp. 1192–1195, 2015.

[77] K. Kikuta and A. Hirose, "Dispersion characteristics of ultra wideband antennas and their radiation patterns," in *2013 International Symposium on Electromagnetic Theory*, pp. 462–465, Hiroshima, Japan, 2013.

[78] Y. Wang, F. Zhang, G. Fang, Y. Ji, S. Ye, and X. Zhang, "A novel ultrawideband exponentially tapered slot antenna of combined electric-magnetic type," *IEEE Antennas and Wireless Propagation Letters*, vol. 15, pp. 1226–1229, 2016.

[79] A. S. Arezoomand, R.-A. Sadeghzadeh, and M. Naser-Moghadasi, "Novel techniques in tapered slot antenna for linearity phase center and gain enhancement," *IEEE Antennas and Wireless Propagation Letters*, vol. 16, pp. 270–273, 2017.

[80] Y. Q. Liu, J. G. Liang, and Y. W. Wang, "Gain-improved double-slot TSA with Y-shaped corrugated edges," *Electronics Letters*, vol. 53, no. 12, pp. 759-760, 2017.

[81] M. Alibakhshi-Kenari, M. Naser-Moghadasi, R. A. Sadeghzadeh, B. S. Virdee, and E. Limiti, "Miniature CRLH-based ultra wideband antenna with gain enhancement for wireless communication applications," *ICT Express*, vol. 2, no. 2, pp. 75–79, 2016.

[82] G. K. Pandey, H. S. Singh, P. K. Bharti, and M. K. Meshram, "Metamaterial based compact antenna design for UWB applications," in *IEEE Region 10 Symposium*, pp. 15–18, Kuala Lumpur, Malaysia, 2014.

[83] H. Xiong, J. S. Hong, and Y. H. Peng, "Impedance bandwidth and gain improvement for microstrip antenna using metamaterials," *Radioengineering*, vol. 21, no. 4, 2012.

[84] H. Xiong, J. S. Hong, Q. Y. Zhu, and D. L. Jin, "Compact ultra-wideband microstrip antenna with metamaterials," *Chinese Physics Letters*, vol. 29, no. 11, 2012.

[85] G. K. Pandey, H. S. Singh, P. K. Bharti, and M. K. Meshram, "Metamaterial-based UWB antenna," *Electronics Letters*, vol. 50, no. 18, pp. 1266–1268, 2014.

[86] J. Baviskar, A. Shah, A. Mulla, A. Baviskar, and P. Dave, "Design and analysis of metamaterial lens incorporated ultra wide band (UWB) antenna," in *2017 IEEE Aerospace Conference*, pp. 1–6, Big Sky, MT, USA, 2017.

[87] M. Alibakhshi-Kenari, M. Naser-Moghadasi, R. Ali Sadeghzadeh, and B. Singh Virdee, "Metamaterial-based antennas for integration in UWB transceivers and portable microwave handsets," *International Journal of RF and Microwave Computer-Aided Engineering*, vol. 26, no. 1, pp. 88–96, 2016.

[88] A. A. Adam, S. K. A. Rahim, K. G. Tan, and A. W. Reza, "Design of 3.1–12 GHz printed elliptical disc monopole antenna with half circular modified ground plane for UWB application," *Wireless Personal Communications*, vol. 69, no. 2, pp. 535–549, 2013.

[89] C.-Y. Huang and W. C. Hsia, "Planar elliptical antenna for ultra-wideband communications," *Electronics Letters*, vol. 41, no. 6, pp. 296-297, 2005.

[90] J.-P. Zhang, Y.-S. Xu, and W.-D. Wang, "Microstrip-fed semi-elliptical dipole antennas for ultrawideband communications," *IEEE Transactions on Antennas and Propagation*, vol. 56, no. 1, pp. 241–244, 2008.

[91] R. Eshtiaghi, J. Nourinia, and C. Ghobadi, "Electromagnetically coupled band-notched elliptical monopole antenna for UWB applications," *IEEE Transactions on Antennas and Propagation*, vol. 58, no. 4, pp. 1397–1402, 2010.

[92] J. Liu, S. Zhong, and K. P. Esselle, "A printed elliptical monopole antenna with modified feeding structure for bandwidth enhancement," *IEEE Transactions on Antennas and Propagation*, vol. 59, no. 2, pp. 667–670, 2011.

[93] L. Sorokosz and W. Zieniutycz, "On the approximation of the UWB dipole elliptical arms with stepped-edge polygon," *IEEE Antennas and Wireless Propagation Letters*, vol. 11, no. 1, pp. 636–639, 2012.

[94] H. G. Foshtami, A. H. Talkhouncheh, and H. Emami, "Wideband log periodic-microstrip antenna with elliptic patches,"

Journal of Information Systems and Telecommunication, vol. 1, no. 2, pp. 113–118, 2013.

[95] A. I. Oni and M. T. Ali, "Design of a compact, low-profile, elliptical patch UWB antenna and performance analysis in vicinity of human layered tissue model for wireless body area network (WBAN) applications," *International Journal of Innovation and Applied Studies*, vol. 8, no. 4, pp. 1770–1781, 2014.

[96] R. Lakshmanan and S. K. Sukumaran, "Flexible ultra wide band antenna for WBAN applications," *Procedia Technology*, vol. 24, pp. 880–887, 2016.

[97] R. Bharadwaj, C. Parini, and A. Alomainy, "Experimental investigation of 3-D human body localization using wearable ultra-wideband antennas," *IEEE Transactions on Antennas and Propagation*, vol. 63, no. 11, pp. 5035–5044, 2015.

[98] L. A. Yimdjo Poffelie, P. J. Soh, S. Yan, and G. A. E. Vandenbosch, "A high-fidelity all-textile UWB antenna with low back radiation for off-body WBAN applications," *IEEE Transactions on Antennas and Propagation*, vol. 64, no. 2, pp. 757–760, 2016.

[99] M. Goudah and M. Y. Yousef, "Bandwidth enhancement techniques comparison for ultra wideband microstrip antennas for wireless application," *Journal of Theoretical and Applied Information Technology*, vol. 35, no. 2, pp. 184–193, 2012.

[100] R. B. V. B. Simorangkir, A. Kiourti, and K. P. Esselle, "UWB wearable antenna with a full ground plane based on PDMS-embedded conductive fabric," *IEEE Antennas and Wireless Propagation Letters*, vol. 17, no. 3, pp. 493–496, 2018.

[101] R. B. V. B. Simorangkir, Y. Yang, and K. P. Esselle, "Robust implementation of flexible wearable antennas with PDMS-embedded conductive fabric," in *12th European Conference on Antennas and Propagation (EuCAP 2018)*, pp. 1–5, London, UK, 2018.

[102] Z. Hamouda, J. L. Wojkiewicz, A. A. Pud, L. Kone, S. Bergheul, and T. Lasri, "Flexible UWB organic antenna for wearable technologies application," *IET Microwaves, Antennas & Propagation*, vol. 12, no. 2, pp. 160–166, 2018.

[103] D. Sarkar, K. V. Srivastava, and K. Saurav, "A compact microstrip-fed triple band-notched UWB monopole antenna," *IEEE Antennas and Wireless Propagation Letters*, vol. 13, pp. 396–399, 2014.

[104] M. Karimiyan-Mohammadabadi, M. A. Dorostkar, F. Shokuohi, M. Shanbeh, and A. Torkan, "Ultra-wideband textile antenna with circular polarization for GPS applications and wireless body area networks," *Journal of Industrial Textiles*, vol. 46, no. 8, pp. 1684–1697, 2016.

[105] P. B. Samal, P. J. Soh, and G. A. E. Vandenbosch, "UWB all-textile antenna with full ground plane for off-body WBAN communications," *IEEE Transactions on Antennas and Propagation*, vol. 62, no. 1, pp. 102–108, 2014.

[106] C. A. Balanis, *Antenna Theory, Analysis and Design*, Wiley, Hoboken, NJ, USA, 3rd edition, 2005.

[107] H. R. Khaleel, "Design and fabrication of compact inkjet printed antennas for integration within flexible and wearable electronics," *IEEE Transactions on Components, Packaging and Manufacturing Technology*, vol. 4, no. 10, pp. 1722–1728, 2014.

[108] M. Ur-Rehman, Q. H. Abbasi, M. Akram, and C. Parini, "Design of band-notched ultra wideband antenna for indoor and wearable wireless communications," *IET Microwaves, Antennas & Propagation*, vol. 9, no. 3, pp. 243–251, 2015.

[109] A. Sani, A. Alomainy, G. Palikaras et al., "Experimental characterization of UWB on-body radio channel in indoor environment considering different antennas," *IEEE Transactions on Antennas and Propagation*, vol. 58, no. 1, pp. 238–241, 2010.

[110] B. B. Malshikare and M. M. Jadhav, "Review paper on design of integrated multi-band UWB antenna for wireless applications," *International Research Journal of Engineering and Technology*, vol. 4, no. 3, pp. 1909–1918, 2017.

[111] P. K. Sharma, P. Singh, and M. Sharma, "A review of microstrip patch antenna for UWB frequency range," *International Journal of Engineering Trends and Technology*, vol. 50, no. 2, pp. 96–102, 2017.

[112] N. Kalambe, D. Thakur, and S. Paul, "Review of microstrip patch antenna using UWB for wireless communication devices," *International Journal of Computer Science and Mobile Computing*, vol. 4, no. 1, pp. 128–133, 2015.

[113] B. Allen, M. Dohler, E. E. Okon, W. Q. Malik, A. K. Brown, and D. J. Edwards, Eds., *Ultra-Wideband Antennas and Propagation: For Communications, Radar and Imaging*, John Wiley & Sons, Inc., Chichester, UK, 2007.

[114] X. Begaud, Ed., *Ultra Wide Band Antennas*, John Wiley & Sons, Inc., London, UK, 2011.

[115] Z. N. Chen and M. Y. W. Chia, *Broadband Planar Antennas: Design and Applications*, John Wiley & Sons, Inc., 2006.

[116] S. K. K. Dash, T. Khan, and A. De, "Dielectric resonator antennas: an application oriented survey," *International Journal of RF and Microwave Computer-Aided Engineering*, vol. 27, no. 3, 2017.

[117] S. Keyrouz and D. Caratelli, "Dielectric resonator antennas: basic concepts, design guidelines, and recent developments at millimeter-wave frequencies," *International Journal of Antennas and Propagation*, vol. 2016, Article ID 6075680, 20 pages, 2016.

[118] H. Wang, W. Zong, N. X. Sun, H. Lin, and S. Li, "Band-notched ultrawide band antenna loaded with ferrite slab," *AIP Advances*, vol. 7, no. 5, 2017.

[119] Y. Shao, Y. Ge, Y. Chen, and H. Zhang, "Compact band-notched UWB dielectric resonator antennas," *Progress In Electromagnetics Research Letters*, vol. 52, pp. 87–92, 2015.

[120] D. Sankaranarayanan, D. Venkatakiran, and B. Mukherjee, "Compact bi-cone dielectric resonator antenna for ultra-wideband applications–a novel geometry explored," *Electromagnetics*, vol. 37, no. 7, pp. 471–481, 2017.

[121] I. Messaoudene, T. A. Denidni, and A. Benghalia, "Low-profile U-shaped DRA for ultra-wideband applications," *International Journal of Microwave and Wireless Technologies*, vol. 9, no. 3, pp. 621–627, 2017.

[122] M. Abedian, S. K. A. Rahim, C. Fumeaux, S. Danesh, Y. C. Lo, and M. H. Jamaluddin, "Compact ultrawideband MIMO dielectric resonator antennas with WLAN band rejection," *IET Microwaves, Antennas & Propagation*, vol. 11, no. 11, pp. 1524–1529, 2017.

[123] R. A. Abd-Alhameed, K. H. Sayidmarie, J. M. Noras, A. S. Abdullah, F. Elmegri, and A. H. Majeed, "Balanced dual-segment cylindrical dielectric resonator antennas for ultra-wideband applications," *IET Microwaves, Antennas & Propagation*, vol. 9, no. 13, pp. 1478–1486, 2015.

[124] M. Abedian, S. K. A. Rahim, S. Danesh, S. Hakimi, L. Y. Cheong, and M. H. Jamaluddin, "Novel design of compact UWB dielectric resonator antenna with dual-band-rejection characteristics for WiMAX/WLAN bands," *IEEE Antennas and Wireless Propagation Letters*, vol. 14, pp. 245–248, 2015.

[125] Y. Wang, N. Wang, T. A. Denidni, Q. Zeng, and G. Wei, "Integrated ultrawideband/narrowband rectangular dielectric resonator antenna for cognitive radio," *IEEE Antennas and Wireless Propagation Letters*, vol. 13, pp. 694–697, 2014.